Article

Developmental Cell

Co-evolving CENP-A and CAL1 Domains Mediate Centromeric CENP-A Deposition across *Drosophila* Species

Graphical Abstract

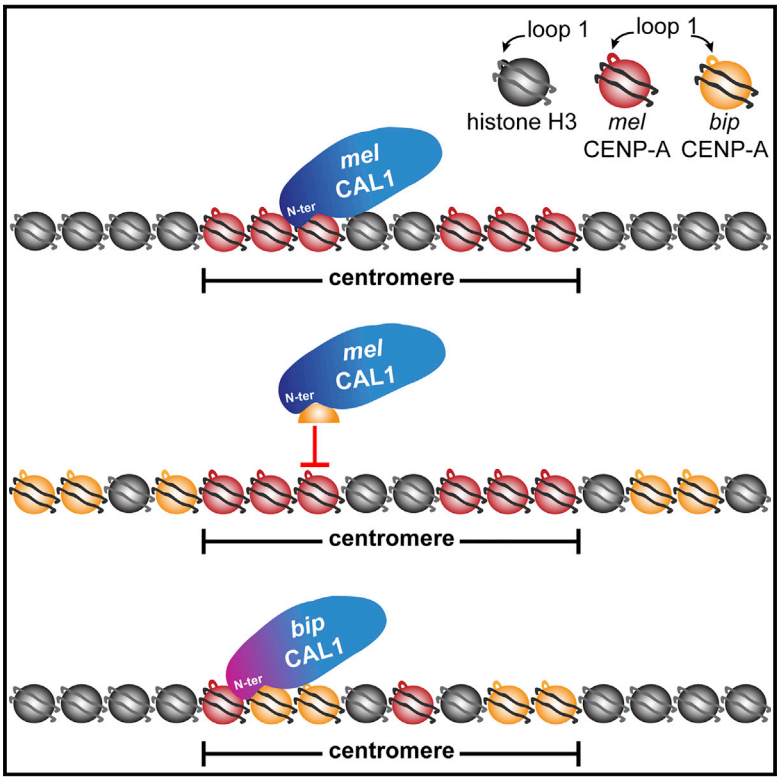

Highlights

- Rapidly evolving CENP-A loop 1 displays species-specific centromere incompatibility
- The incompatibility reflects a mismatch between CENP-A and its assembly factor CAL1
- The N terminus of CAL1 mediates CENP-A assembly in a lineage-specific manner
- Compatible CENP-A loop 1 and CAL1 N terminus are critical for CENP-A deposition

Authors

Leah Rosin, Barbara G. Mellone

Correspondence

barbara.mellone@uconn.edu

In Brief

Although the process of chromosome segregation is highly conserved, centromeres and the centromeric histone, CENP-A, are rapidly evolving. Rosin and Mellone find that *Drosophila* CENP-A evolves in concert with its chaperone, CAL1, and deposition of CENP-A onto chromatin depends on compatibility with CAL1, rather than centromeric sequences.

Rosin & Mellone, 2016, Developmental Cell *37*, 136–147
April 18, 2016
http://dx.doi.org/10.1016/j.devcel.2016.03.021

CellPress

Developmental Cell
Article

Co-evolving CENP-A and CAL1 Domains Mediate Centromeric CENP-A Deposition across *Drosophila* Species

Leah Rosin[1] and Barbara G. Mellone[1,2,*]
[1]Department of Molecular and Cell Biology
[2]Institute for Systems Genomics
University of Connecticut, Storrs, CT 06269, USA
*Correspondence: barbara.mellone@uconn.edu
http://dx.doi.org/10.1016/j.devcel.2016.03.021

SUMMARY

Centromeres mediate the conserved process of chromosome segregation, yet centromeric DNA and the centromeric histone, CENP-A, are rapidly evolving. The rapid evolution of *Drosophila* CENP-A loop 1 (L1) is thought to modulate the DNA-binding preferences of CENP-A to counteract centromere drive, the preferential transmission of chromosomes with expanded centromeric satellites. Consistent with this model, CENP-A from *Drosophila bipectinata* (*bip*) cannot localize to *Drosophila melanogaster* (*mel*) centromeres. We show that this result is due to the inability of the *mel* CENP-A chaperone, CAL1, to deposit *bip* CENP-A into chromatin. Co-expression of *bip* CENP-A and *bip* CAL1 in *mel* cells restores centromeric localization, and similar findings apply to other *Drosophila* species. We identify two co-evolving regions, CENP-A L1 and the CAL1 N terminus, as critical for lineage-specific CENP-A incorporation. Collectively, our data show that the rapid evolution of L1 modulates CAL1-mediated CENP-A assembly, suggesting an alternative mechanism for the suppression of centromere drive.

INTRODUCTION

Centromeres are essential chromosomal structures to which kinetochore proteins and microtubules are recruited during cell division to mediate the accurate distribution of genetic material. While centromere function is highly conserved, centromere size and structure vary greatly between organisms (Fukagawa and Earnshaw, 2014). In complex eukaryotes, the specific DNA sequences found at centromeres are neither necessary nor sufficient for centromere formation (Choo, 2000; Karpen and Allshire, 1997), and centromeres are epigenetically defined by the presence of a centromere-specific histone H3 variant called CENP-A (also called CID in *Drosophila*) (Earnshaw and Rothfield, 1985; Karpen and Allshire, 1997).

Accurate CENP-A deposition is mediated by specific CENP-A assembly factors (or chaperones). While yeast and humans harbor CENP-A chaperones with common ancestry (called Scm3 and HJURP, respectively) (Bernad et al., 2011; Camahort et al., 2007; Dunleavy et al., 2009; Foltz et al., 2009; Mizuguchi et al., 2007; Pidoux et al., 2009; Sanchez-Pulido et al., 2009), *Drosophila* employ an evolutionarily distinct CENP-A chaperone called CAL1 (Chen et al., 2014; Erhardt et al., 2008; Phansalkar et al., 2012).

Despite the universally conserved function of centromeres in maintaining genome integrity, both CENP-A (Cooper and Henikoff, 2004; Finseth et al., 2015; Henikoff et al., 2001; Malik and Henikoff, 2001; Malik et al., 2002; Ravi et al., 2010; Schueler et al., 2010; Talbert et al., 2002; Zedek and Bureš, 2012) and centromeric DNA (Melters et al., 2013) are rapidly evolving. This paradox has been explained by the centromere drive hypothesis, which proposes that CENP-A adaptively evolves to maintain meiotic parity by modulating its DNA-binding preferences to counteract the transmission advantage gained by satellite expansion in female meiosis (Henikoff and Malik, 2002; Malik and Henikoff, 2002). In support of this model, adaptive evolution has been observed in both the N-terminal tail and loop 1 (L1) of CENP-A (Cooper and Henikoff, 2004; Finseth et al., 2015; Henikoff et al., 2001; Malik and Henikoff, 2001; Malik et al., 2002; Ravi et al., 2010; Schueler et al., 2010; Talbert et al., 2002; Zedek and Bureš, 2012), both of which are putative DNA-binding regions (Luger et al., 1997; Malik et al., 2002; Vermaak et al., 2002), in plants and animals. The role of CENP-A chaperones in this evolutionary "arms race" has yet to be explored.

Somewhat surprising is the fact that, while *Drosophila* CENP-A is adaptively evolving (Malik and Henikoff, 2001; Malik et al., 2002), its chaperone CAL1 is highly conserved across both the N-terminal domain, which interacts with CENP-A, and the C-terminal domain, which interacts with CENP-C (Chen et al., 2014; Phansalkar et al., 2012; Schittenhelm et al., 2010). How CAL1 is able to interact with and deposit rapidly evolving CENP-A orthologs, given their different rates of evolution, is unknown.

While several lines of evidence support the rapid evolution of both centromeric DNA and CENP-A in many species (Melters et al., 2013), and also the influence of centromere expansion on meiotic segregation distortion (Chmátal et al., 2014; Daniel, 2002; Fishman and Saunders, 2008; Fishman and Willis, 2005; Pardo-Manuel de Villena and Sapienza, 2001; Wyttenbach et al., 1998), biological data supporting a direct correlation between the evolution of centromeric DNA and CENP-A (the second step in the centromere drive hypothesis (Malik, 2009; Malik

and Henikoff, 2002)) are lacking. However, one striking experimental observation supporting centromere drive is that CENP-A from *Drosophila bipectinata* (*bip*) expressed in *Drosophila melanogaster* (*mel*) tissue culture cells is unable to localize to *mel* centromeres (Vermaak et al., 2002). This incompatibility is the result of specific amino acid changes in L1 of CENP-A (Vermaak et al., 2002). Because L1 of histone H3 has been shown to interact with DNA (Luger et al., 1997), it was proposed that L1 of CENP-A is adaptively evolving with centromeric DNA satellites to suppress centromere drive (Malik and Henikoff, 2001; Vermaak et al., 2002). However, recent structural studies of human CENP-A octamers and tetramers suggest that L1 of CENP-A does not interact with DNA, and instead is exposed in the nucleosome particle (Sekulic et al., 2010; Tachiwana et al., 2012). Interestingly, in yeast and humans, a domain encompassing L1 known as the CENP-A targeting domain (CATD) is recognized by the assembly factors Scm3 and HJURP, respectively (Bassett et al., 2012; Cho and Harrison, 2011). The CATD is sufficient to confer centromeric localization to histone H3 in both yeast and humans (Black et al., 2004; Shelby et al., 1997). However, the corresponding region of *Drosophila* CENP-A is not sufficient for the centromeric localization of histone H3 in flies (Moreno-Moreno et al., 2011). How CAL1 recognizes *Drosophila* CENP-A is unknown.

Here, we use evolutionary cell biology to investigate the relationship between centromere divergence and CENP-A assembly in *Drosophila*. We reveal that a functional interplay between CAL1 and L1 of CENP-A is both necessary and sufficient for the deposition of orthologous CENP-A proteins at *mel* native centromeres as well as for de novo CENP-A recruitment to an ectopic locus. Successful CENP-A incorporation requires that L1 and the CAL1 N terminus are compatible, demonstrating that these two domains evolve in concert. These data challenge previous models of centromere drive involving the adaptive evolution of L1 with centromeric DNA in *Drosophila* and suggest that the evolution of L1 may instead mediate CENP-A centromeric deposition by CAL1.

RESULTS

Inter-species Centromeric Localization of *Drosophila* CENP-A Orthologs Can Only Partially Be Explained by Phylogenetic Distance

Loop 1 (L1) of CENP-A has long been proposed to be adaptively evolving with centromeric DNA in an "arms race" akin to that occurring between viruses and their hosts (Malik and Henikoff, 2001; Vermaak et al., 2002). A previous study tested the ability of CENP-A orthologs from *Drosophila simulans* (*sim*), *Drosophila erecta* (*ere*), *Drosophila lutescens* (*lut*), *Drosophila bipectinata* (*bip*), and *Drosophila pseudoobscura* (*pse*) to localize to centromeres in *D. melanogaster* (*mel*) cultured Kc cells, to identify CENP-A centromere-targeting motifs (Vermaak et al., 2002). While centromeric localization was observed for CENP-A orthologs from most species, *bip* CENP-A failed to localize to *mel* centromeres (12 Ma diverged; Figure 1A), despite the fact that the more divergent *pse* CENP-A (30 Ma diverged; Figure 1A) was able to localize (Vermaak et al., 2002).

To better understand the relationship between centromeric localization of CENP-A orthologs in *mel* cells and their phylogenetic distance from *mel*, we tested additional CENP-A orthologs from four evolutionarily intermediate species between *mel* and *bip* (*Drosophila takahashii* [*tak*], *Drosophila rhopolia* [*rho*], *Drosophila kikkawai* [*kik*], and *Drosophila ananassae* [*ana*]), and from three more distant species (*Drosophila miranda* [*mir*], *Drosophila willistoni* [*wil*], and *Drosophila virilis* [*vir*]; Figure 1A), along with *mel*, *sim*, *ere*, *bip*, and *pse* as in the original study (Vermaak et al., 2002) for their ability to localize to *mel* centromeres (Figures 1B–1D and S1). GFP-tagged CENP-A orthologs from these 11 *Drosophila* species, as well as *mel* histone H3.1 as a control, were transiently expressed in *mel* Schneider 2 (S2) cells (Figure 1B). The localization of GFP-CENP-A orthologs was assessed by immunofluorescence (IF) on interphase S2 cells using anti-GFP and anti-*mel* CENP-A antibodies, which are specific to *mel* CENP-A and are used as a marker for *mel* centromeres (Figures 1C and S2).

Localization to *mel* centromeres was observed for those CENP-A orthologs that are most closely related to *mel*, namely *sim*, *ere*, *tak*, and *rho*. In contrast, *bip*, *wil*, and *vir* CENP-A failed to localize, resulting in diffuse GFP signal ($p < 0.0001$). *kik* and *ana* CENP-A partially localized to *mel* S2 centromeres, displaying both centromeric and diffuse GFP signal ($p = 0.005$ for *kik* and $p = 0.0003$ for *ana*). Interestingly, centromeric localization was also observed for CENP-A orthologs from the *obscura* group (*pse* and *mir*; 55% [$p = 0.002$] and 70% centromeric, respectively; Figures 1C, 1D and S1), which is more divergent from *mel* than either the *montium* or *ananassae* subgroups (Figure 1A). The same localization pattern was observed with hemagglutinin (HA)-tagged CENP-A orthologs (Figures S3A–S3C), indicating that the presence of the GFP tag does not interfere with centromeric localization. Together, these findings confirm and expand upon previous work (Vermaak et al., 2002), and demonstrate that the CENP-A localization pathway is conserved between the *melanogaster* and *obscura* groups, but has diverged in the *ananassae* subgroup. Additionally, the CENP-A localization pathway is not conserved in more divergent lineages (e.g., *wil* and *vir*).

Unlike the rapid degradation of mislocalized *mel* CENP-A after pulse induction (Heun et al., 2006; Olszak et al., 2011), which requires the F-box protein PPA and the CATD (Moreno-Moreno et al., 2011), *bip* and *wil* CENP-A proteins appear to persist stably, resulting in higher protein levels compared with those of centromere-localizing CENP-A orthologs (Figure 1C). Perhaps *mel* PPA cannot recognize *bip* and *wil* CENP-A due to their divergent L1 (Vermaak et al., 2002), which is part of the CATD.

We next asked whether the localization of CENP-A orthologs followed a similar pattern at the centromeres of *sim*, a species closely related to *mel* (Figure 1A). Transient transfection with *sim*, *mel*, *ere*, *bip*, and *pse* GFP-CENP-A constructs in *sim* M-19 tissue culture cells was followed by IF with anti-GFP and anti-CENP-C antibodies, which recognize *sim* CENP-C providing a centromere marker (Figures S3D and S3E). Similar to the localization results in *mel* cells, *mel*, *ere*, and *pse* CENP-A localize to *sim* centromeres, while *bip* CENP-A does not (Figures S3D and S3E). These results show that the centromeric localization of CENP-A orthologs to *mel* and *sim* centromeres can only partially be explained by phylogenetic distance and that the branch containing the *ananassae* subgroup is evolving on a separate evolutionary trajectory from that of other close

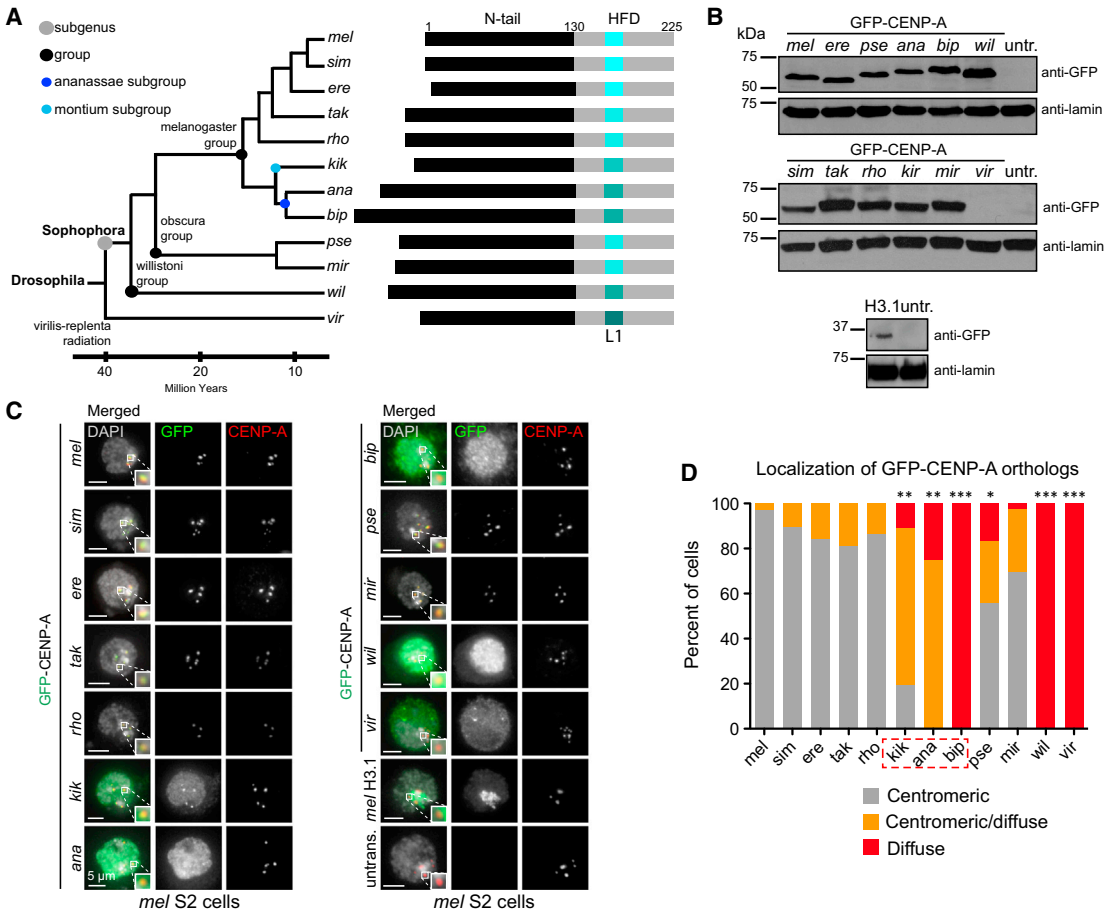

Figure 1. Inter-species Centromeric Localization of *Drosophila* CENP-A Orthologs Can Only Partially Be Explained by Phylogenetic Distance

(A) Left: phylogenetic tree of the *Drosophila* species analyzed in this study (*mel*, *D. melanogaster*; *sim*, *D. simulans*; *ere*, *D. erecta*; *tak*, *D. takahashii*; *rho*, *D. rhopalia*; *kik*, *D. kikkawai*; *ana*, *D. ananassae*; *bip*, *D. bipectinata*; *pse*, *D. pseudoobscura*; *mir*, *D. miranda*; *wil*, *D. willistoni*; *vir*, *D. virilis*). Divergence time and phylogenetic grouping based on Flybase. Right: schematic of CENP-A orthologs from indicated species showing relative differences in protein size. The N terminus is shown in black and the histone fold domain (HFD) is shown in gray. Loop 1 (L1) is shown shades of aqua indicative of divergence in L1. Numbers indicate amino acid positions.

(B) Western blots with anti-GFP (top) and anti-lamin (loading control, bottom) antibodies of total cell extracts showing the expression of GFP-CENP-A orthologs in S2 cells used in (C) and (D). The expression of *vir* GFP-CENP-A was too low to visualize by western blot.

(C) Immunofluorescence (IF) images of *mel* S2 interphase cells transiently expressing *Drosophila* GFP-CENP-A orthologs. Images where endogenous CENP-A is present were chosen to visualize the location of the centromere. DAPI is shown in gray, GFP in green, and mel CENP-A in red. Zoomed insets show representative centromeres with merged colors.

(D) Quantification of (C). Images were manually classified as having either centromeric localization of GFP (gray bars), diffuse localization of GFP (red bars), or centromeric/diffuse (orange bars). Number of transfected cells quantified for each ortholog: 97 for *mel*, 114 for *sim*, 94 for *ere*, 58 for *tak*, 67 for *rho*, 36 for *kik*, 52 for *ana*, 143 for *bip*, 90 for *pse*, 212 for *mir*, 68 for *wil*, and 35 for *vir*. Fisher's two-tailed test p values were ***p < 0.0001 for *bip* CENP-A, *wil* CENP-A, and *vir* CENP-A; **p = 0.0003 for *ana*; **p = 0.005 for *kik*; and *p = 0.002 for *pse* CENP-A compared with *mel* CENP-A. These data were confirmed by one biological replicate with GFP-tagged constructs, and two additional replicates with HA-tagged constructs.

See also Figures S1–S3.

lineages. Furthermore, these experiments demonstrate that the incompatibility between CENP-A and the centromere is not unique to the *bip*/*mel* species pair.

D. melanogaster CAL1 Cannot Recruit *D. bipectinata* CENP-A at an Ectopic Locus

The mislocalization of *bip* CENP-A in *mel* cells is due to key amino acid changes between L1 of *bip* and *mel* CENP-A (Vermaak et al., 2002). It was originally proposed that this variation in CENP-A L1 is indicative of adaptive evolution with centromeric DNA to suppress drive (Malik and Henikoff, 2001; Vermaak et al., 2002). However, another possibility is that *bip* CENP-A may be co-evolving (defined here as undergoing coordinated protein evolution) with its loading factor CAL1 (Chen et al., 2014), and that the failure of *bip* CENP-A to localize to *mel* centromeres could be due to an incompatibility with *mel* CAL1.

We investigated this possibility by first determining whether *bip* CENP-A can physically interact with *mel* CAL1. Immunoprecipitations (IPs) with anti-CAL1 antibodies coupled to beads were performed in two separate chromatin extracts that

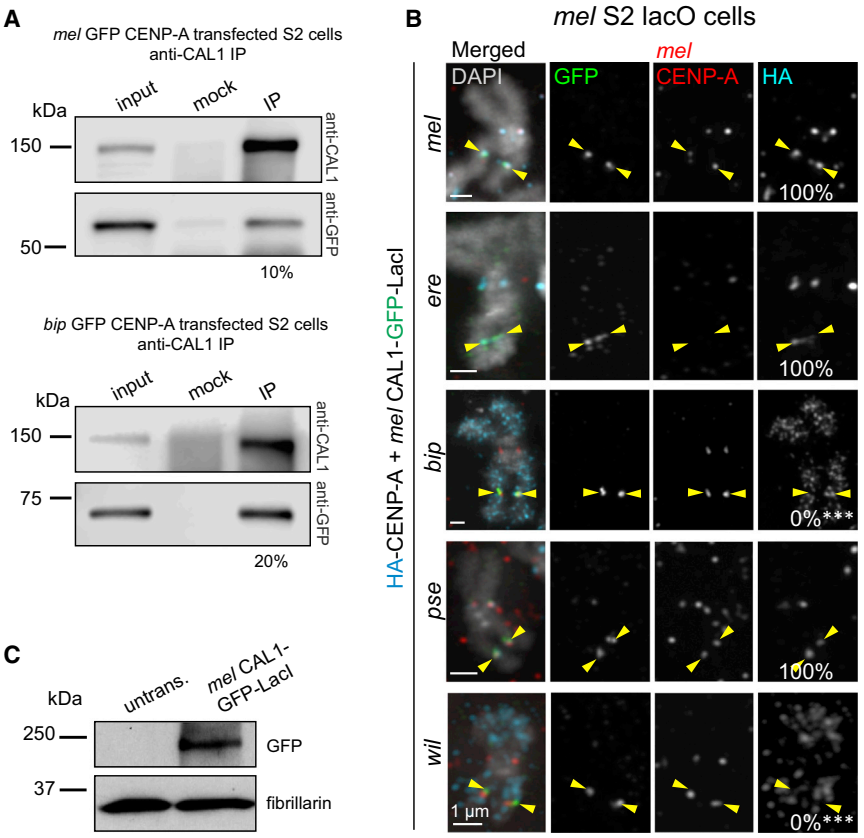

Figure 2. *D. melanogaster* CAL1 Cannot Recruit *D. bipectinata* CENP-A to an Ectopic Locus

(A) Western blots of IPs with anti-CAL1 antibodies from nuclear extracts transiently expressing *mel* GFP-CENP-A (top) or *bip* GFP-CENP-A (bottom). IP was confirmed using anti-CAL1 antibody (top blot). Presence of GFP-CENP-A in CAL1 pull-downs was detected with anti-GFP antibody (bottom blot). Shown is the percentage of immunoprecipitated GFP-CENP-A relative to input.

(B) Representative IF images of metaphase chromosome spreads from *mel* S2 lacO cells transiently co-expressing *mel* CAL1-GFP-LacI and HA-CENP-A orthologs: *mel* (top); *ere* (second); *bip* (third); *pse* (fourth); and *wil* (bottom). Chromosome spreads were quantified for the presence of HA-CENP-A at the lacO site (percentage shown in right column). Endogenous *mel* CENP-A is shown in red, HA in aqua, GFP in green, and DAPI in gray. Note that *mel* CENP-A antibodies are specific for this species and that upon expression of CENP-A orthologs that localize to *mel* centromeres, endogenous CENP-A levels decrease (e.g., *ere* CENP-A; see also Figure S2). This is not observed for *mel* HA-CENP-A, as *mel* CENP-A antibodies recognize this tagged protein. ***$p < 0.0001$ (Fisher's two-tailed test) for *bip* or *wil* CENP-A compared with *mel* CENP-A recruitment at the lacO. n = 13 spreads for *mel* CENP-A recruitment, 8 for *ere*, 11 for *bip*, 15 for *pse*, and 8 for *wil*. Yellow arrowheads indicate the lacO array. These results were confirmed by one biological replicate with the CAL1-GFP-LacI construct, and two biological replicates with GFP-CENP-A and CAL1-LacI constructs (data not shown).

(C) Western blots with anti-GFP (top) and anti-fibrillarin (loading control, bottom) antibodies of whole-cell extracts showing the expression of induced *mel* CAL1-GFP-LacI in lacO cells shown in (B).

contained normalized amounts of *mel* or *bip* GFP-CENP-A. Quantification of GFP-CENP-A western blot bands indicated that *mel* CAL1 pulled down approximately 10% of *mel* GFP-CENP-A and 20% of *bip* GFP-CENP-A relative to the respective inputs. These experiments indicate that *mel* CAL1 can form a complex with *bip* GFP-CENP-A at least as efficiently as with *mel* GFP-CENP-A and that there is no incompatibility as far as physical interaction between these two proteins is concerned (Figure 2A).

We next investigated whether the ability of *mel* CAL1 to interact with *bip* CENP-A enables its deposition into chromatin. We turned to an ectopic tethering assay, which allows us to interrogate the functional relationship between *mel* CAL1 and CENP-A from *bip* and from other representative species without centromeric DNA as a contributing factor. Tethering *mel* CAL1 via the *lac* repressor, LacI, at a lacO array stably integrated within a chromosome arm leads to the stable incorporation of *mel* CENP-A (Chen et al., 2014). We co-expressed HA-tagged *mel*, *ere*, *pse*, *bip*, or *wil* CENP-A and an inducible *mel* CAL1 tagged with GFP and LacI (Figures 2B and 2C). After 24 hr induction of *mel* CAL1-GFP-LacI, recruitment of HA-CENP-A orthologs to the lacO site was analyzed by IF with anti-HA, anti-GFP (to detect CAL1-GFP-LacI at the lacO site), and anti-*mel* CENP-A antibodies (to visualize the *mel* endogenous centromere) on metaphase chromosomes. This analysis showed that *mel* CAL1-GFP-LacI successfully recruits *sim*, *ere*, and *pse* CENP-A to the lacO site (Figure 2B). In contrast, *bip* and *wil* CENP-A are not recruited to the lacO site and localize all along the chromosome arms in a pattern reminiscent of *mel* CENP-A overexpression ((Heun et al., 2006); Figure 2B). These experiments suggest that, although *mel* CAL1 can interact with *bip* CENP-A (Figure 2A), this interaction is not functional, i.e., *mel* CAL1 cannot deposit *bip* CENP-A into chromatin (Figure 2B). Furthermore, they show that the successful ectopic targeting of CENP-A from *sim*, *ere*, and *pse* reflects their competency to localize to *mel* endogenous centromeres (Figure 1C). These data also demonstrate that the overexpression of *mel* CAL1-GFP-LacI is not sufficient to promote the centromeric or lacO targeting of *bip* and *wil* CENP-A.

Co-expression of CAL1 and CENP-A Ortholog Pairs Rescues Centromeric Localization

While our ectopic targeting assays suggest that *mel* CAL1 cannot incorporate *bip* or *wil* CENP-A into chromatin at the lacO site, they did not allow us to discriminate between defective recruitment by *mel* CAL1 or an incompatibility between *bip* or *wil* CENP-A and DNA sequences present at *mel* endogenous centromeres. If the failure of *bip* CENP-A to associate with *mel*

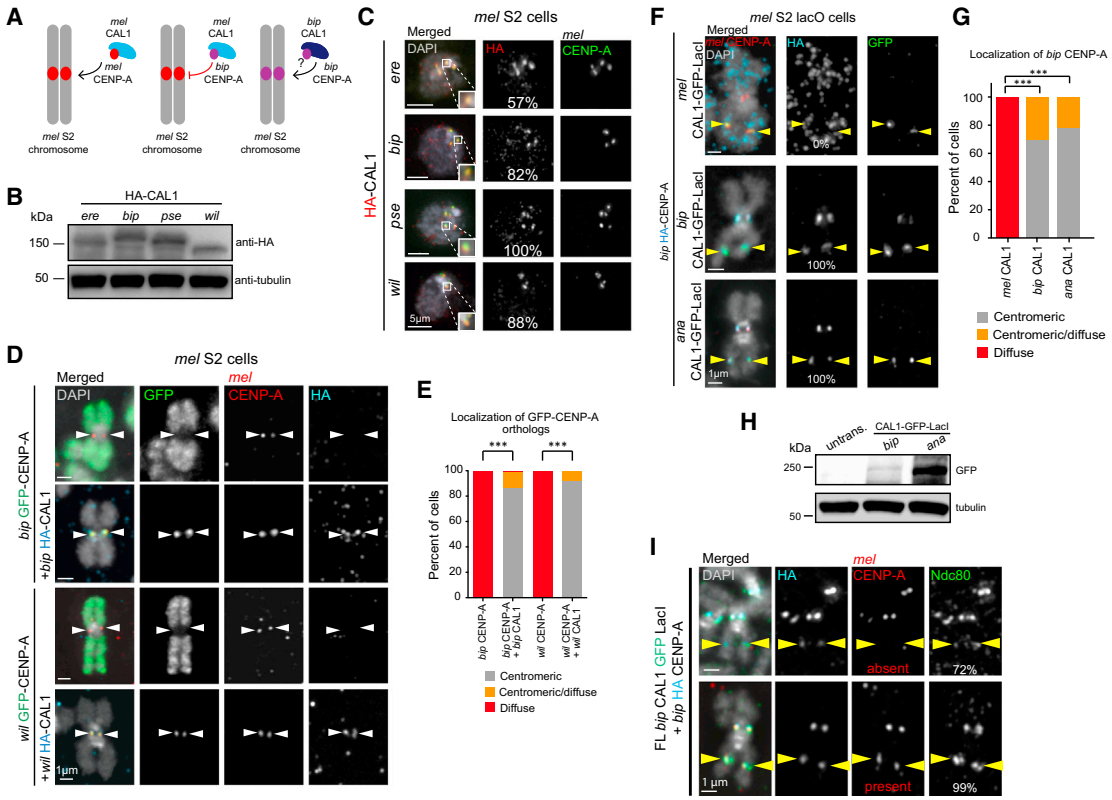

Figure 3. Co-expression of CAL1 and CENP-A Ortholog Pairs Rescues Centromeric Localization

(A) Schematic of the experiments testing whether co-expression of *bip* CAL1 and *bip* CENP-A can result in the localization of *bip* CENP-A to *mel* centromeres.

(B) Western blots of whole-cell extracts showing expression of HA-CAL1 constructs. Top: anti-HA. Bottom: anti-tubulin (loading control).

(C) Representative IF images of interphase *mel* S2 cells transiently expressing HA-CAL1 orthologs. DAPI is shown in gray, HA in red, and *mel* CENP-A in green. The percentage of cells with centromeric HA signal is indicated in the middle column. Zoomed panels show representative centromeres with merged colors.

(D) Representative IF images of metaphase chromosome spreads from S2 cells transiently expressing *bip* or *wil* GFP-CENP-A alone (first and third rows, respectively), *bip* GFP-CENP-A and *bip* HA-CAL1 (second row), or *wil* GFP-CENP-A and *wil* HA-CAL1 (fourth row). DAPI is shown in gray, GFP in green, HA in aqua, and *mel* CENP-A in red. White arrowheads indicate the position of the centromere.

(E) Quantification of the IF shown in (D). Chromosome spreads were manually classified as having either centromeric (gray bars), diffuse (red), or centromeric/diffuse (orange) GFP signal. n = 29 spreads for *bip* CENP-A alone, 73 for *bip* CENP-A with *bip* CAL1, 27 for *wil* CENP-A alone, and 51 for *wil* CENP-A with *wil* CAL1. ***$p < 0.0001$ (Fisher's two-tailed test) for the centromeric localization of *bip* and *wil* CENP-A with and without CAL1. These data were confirmed by one biological replicate using HA-tagged CAL1 constructs (data not shown), and two biological replicates using CAL1-GFP-LacI and HA-CENP-A constructs (see F in this figure for *bip*, and data not shown for *wil*). See also Figures S4 and S5.

(F) Representative IF images of metaphase chromosome spreads from *mel* lacO S2 cells transiently co-expressing *mel*, *bip*, *or ana* CAL1-GFP-LacI (first, second, or third row, respectively), and *bip* HA-CENP-A. GFP is shown in green, HA in aqua, *mel* CENP-A in red, and DAPI in gray. Yellow arrowheads indicate the position of the lacO site.

(G) Quantification of the images shown in (F). Cells were manually classified as having either exclusively centromeric GFP signal (gray bars), diffuse GFP signal (red bars), or centromeric and diffuse GFP signal (orange bars). n ≥ 30 cells per condition. These data were confirmed by two biological replicates (data not shown). ***$p < 0.0001$ (Fisher's two-tailed test).

(H) Western blots with anti-GFP (top) and anti-tubulin (loading control, bottom) antibodies of whole-cell extracts showing the expression of induced *bip* and *ana* CAL1-GFP-LacI in lacO cells in F.

(I) Representative IF images of metaphase chromosome spreads from *mel* lacO S2 cells transiently co-expressing *bip* CAL1-GFP-LacI and *bip* HA-CENP-A (aqua) showing the lacO recruitment of endogenous *mel* CENP-A (red) and the outer kinetochore protein Ndc80 (green). GFP fluorescence was quenched with 100% ethanol. DAPI is shown in gray. Percentage of CENP-A positive (*bip*, or *mel* and *bip*) lacO arrays with Ndc80 is indicated in the right column. Yellow arrowheads mark the position of lacO site. These data represent the average of three experiments (two technical replicates and one biological replicate). n = 40 HA-positive cells.

centromeres is solely due to an incompatible assembly factor (*mel* CAL1), then supplying *bip* CAL1 should rescue the centromeric localization of *bip* CENP-A in *mel* cells (Figure 3A).

To test this, we first needed to determine whether *bip* CAL1 can localize to *mel* centromeres, a necessary prerequisite for the deposition of CENP-A at this location (Chen et al., 2014; Erhardt et al., 2008). HA-tagged *bip*, *ere*, *pse*, or *wil* CAL1 were transiently expressed in S2 cells (Figure 3B). IF with anti-HA and anti-*mel* CENP-A antibodies showed that all of the HA-CAL1 orthologs localize to *mel* centromeres in at least 50% of cells (Figure 3C). Since CAL1 is recruited to centromeres by CENP-C (Chen et al., 2014), these data suggest that the

CENP-C/CAL1 interaction is conserved between *mel* and *bip* and, more generally, across the *Drosophila* phylogeny. The observation that the C terminus of CAL1, which interacts with CENP-C (Chen et al., 2014; Schittenhelm et al., 2010), is under purifying selection (Phansalkar et al., 2012) is consistent with this hypothesis.

Next, we tested whether supplying *bip* CAL1 enables *bip* CENP-A to localize to *mel* centromeres by transiently transfecting *mel* S2 cells with *bip* GFP-CENP-A and *bip* HA-CAL1 constructs (Figure 3D). IF with anti-HA, anti-GFP, and anti-*mel* CENP-A antibodies on metaphase spreads showed that centromeric targeting of *bip* CENP-A is completely restored in 86% of cells and partially restored in 12% (Figures 3D and 3E). Furthermore, the observation that the centromeric *bip* GFP-CENP-A IF signal is resistant to salt extraction demonstrates that it is incorporated into chromatin (Figure S4). The centromeric and lacO targeting of *bip* CENP-A was also obtained with the reversed tags: *bip* CAL1-GFP-LacI with *bip* HA-CENP-A (Figures 3F–3H).

To test whether the functional interaction between *bip* CAL1 and CENP-A is lineage specific or species specific, we co-expressed *bip* HA-CENP-A with *ana* CAL1-GFP-LacI in *mel* lacO cells and assessed the recruitment of *bip* HA-CENP-A at the lacO site by IF with anti-HA, anti-GFP, and anti-*mel* CENP-A antibodies on metaphase spreads. We found that *ana* CAL1 is competent for *bip* CENP-A deposition at both *mel* centromeres (78% fully centromeric and 22% partially centromeric) and the lacO site (100%; Figures 3F–3H). We conclude that the presence of a lineage-specific CAL1 partner can also promote the centromeric targeting of *bip* CENP-A in *mel* cells.

To determine whether the centromeric localization of *bip* CENP-A can also occur in *sim* cells, we co-expressed *bip* CENP-A and *bip* CAL1 in M-19 cells and observed *bip* CENP-A centromeric targeting in 56% of cells (Figures S5A and S5B). These results are consistent with our findings in *mel* cells (Figures 3D and 3E) and demonstrate that a similar CENP-A loading defect is present between *bip* CENP-A and *sim* CAL1.

Next, we investigated whether a similar mechanism underlies the defective localization of the more divergent *wil* CENP-A to *mel* centromeres. We transiently co-expressed *wil* GFP-CENP-A with *wil* HA-CAL1, and assessed centromeric localization by IF. As with *bip* CENP-A, we observed exclusively centromeric localization of *wil* CENP-A in 92% of cells and partial localization in 8% (Figures 3D and 3E). We conclude that even CENP-A from a species almost 40 Ma diverged from *mel* can localize to *mel* centromeres as long as a compatible CAL1 partner is present.

Given the ability of the *bip* CENP-A/CAL1 complex to localize to *mel* centromeres, we next asked if this complex can initiate *mel* kinetochore assembly by assessing the recruitment of the outer kinetochore component Ndc80 (Meraldi et al., 2006). *Bip* CAL1-GFP-LacI was tethered to the lacO array in *mel* cells expressing *bip* HA-CENP-A followed by IF with anti-HA, anti-*mel* CENP-A, and anti-Ndc80 on metaphase spreads. We noticed that the full-length *bip* CAL1-GFP-LacI construct recruited *mel* CENP-A to the lacO site in approximately 50% of chromosome spreads ($p < 0.0001$ compared with *mel* CAL1-GFP-LacI recruitment of *bip* CENP-A), suggesting that there is more functional conservation between *mel* and *bip* CAL1 than between *mel* and *bip* CENP-A. By scoring *bip* CENP-A-positive lacO sites for both the presence or absence of *mel* CENP-A and Ndc80, we found that *bip* CAL1-GFP-LacI can recruit Ndc80 even when *mel* CENP-A is absent or nearly undetectable (72% compared with 99% when *mel* CENP-A is present at the lacO site [$p = 0.2$]; Figure 3I). We conclude that the *bip* CENP-A/CAL1 complex can mediate *mel* kinetochore formation, bypassing the requirement for *mel* CENP-A. These results may explain why the co-expression of *bip* CAL1 and *bip* CENP-A does not negatively affect chromosome segregation, whereas the expression of *ere* CENP-A does (Figure S6). In plants, too, centromeric localization of CENP-A orthologs is not a predictor of whether they can form functional kinetochores (Ravi et al., 2010).

CAL1 Recognizes CENP-A via L1

It has previously been shown that replacing L1 of *mel* CENP-A with the homologous region of *bip* CENP-A results in a loss of centromeric localization, while substituting L1 of *bip* CENP-A with *mel* L1 results in a gain of centromeric localization (Vermaak et al., 2002). Based on these data and our findings so far, we hypothesized that L1 of CENP-A could mediate the functional interaction with CAL1, and that the divergence of *bip* L1 (Vermaak et al., 2002) results in the failure of *mel* CAL1 to properly deposit *bip* CENP-A into chromatin.

To test this hypothesis, we generated a GFP-tagged *mel* CENP-A chimera containing L1 from *bip* CENP-A (*mel* CENP-A^{bipL1}; Figure 4A) and transiently expressed it in *mel* S2 cells (Figure 4B) with and without *bip* CAL1. When expressed alone, *mel* CENP-A^{bipL1} is mislocalized in all mitotic chromosome spreads (0% centromeric). However, when *mel* CENP-A^{bipL1} is co-expressed with *bip* CAL1, it becomes centromeric in all spreads (100%; Figure 4C). A similar pattern was observed in interphase cells, where *mel* CENP-A^{bipL1} is mislocalized or only partially centromeric (82% and 19% of cells, respectively) when expressed alone, but becomes fully centromeric when co-expressed with *bip* CAL1 (90%; Figures 4D and 4E). Thus, the mislocalization of the *mel* CENP-A^{bipL1} chimera is the result of some sort of dysfunction occurring within the *bip* CENP-A L1 and the *mel* CAL1 complex.

If L1 is critical for the function of CENP-A and CAL1 complexes, the recruitment of *bip* CENP-A to the lacO site is expected to be restored if L1 from *bip* CENP-A is replaced with L1 from *mel* CENP-A (*bip* CENP-A^{melL1} chimera; Figure 4F) (Vermaak et al., 2002). To test this prediction, we transiently transfected *mel* CAL1-GFP-LacI and HA-tagged *bip* CENP-A^{melL1} in S2 lacO cells (Figure 4G), and assessed recruitment to the lacO site by IF on metaphase spreads. In agreement with previous data (Vermaak et al., 2002), *bip* CENP-A^{melL1} chimera localizes to *mel* centromeres. Furthermore, *mel* CAL1-GFP-LacI recruits *bip* CENP-A^{melL1} to the lacO array with the same efficiency as *mel* CENP-A (100%; Figure 4H) (Chen et al., 2014). These data demonstrate that the centromeric localization gained by the addition of *mel* L1 to *bip* CENP-A is a result of its restored ability to be incorporated into chromatin by *mel* CAL1.

Identification of CAL1 Residues Co-evolving with CENP-A L1

Having determined that the divergence between the L1 of *mel* and *bip* CENP-A leads to defective centromeric deposition of *bip* CENP-A by *mel* CAL1, we sought to identify the corresponding

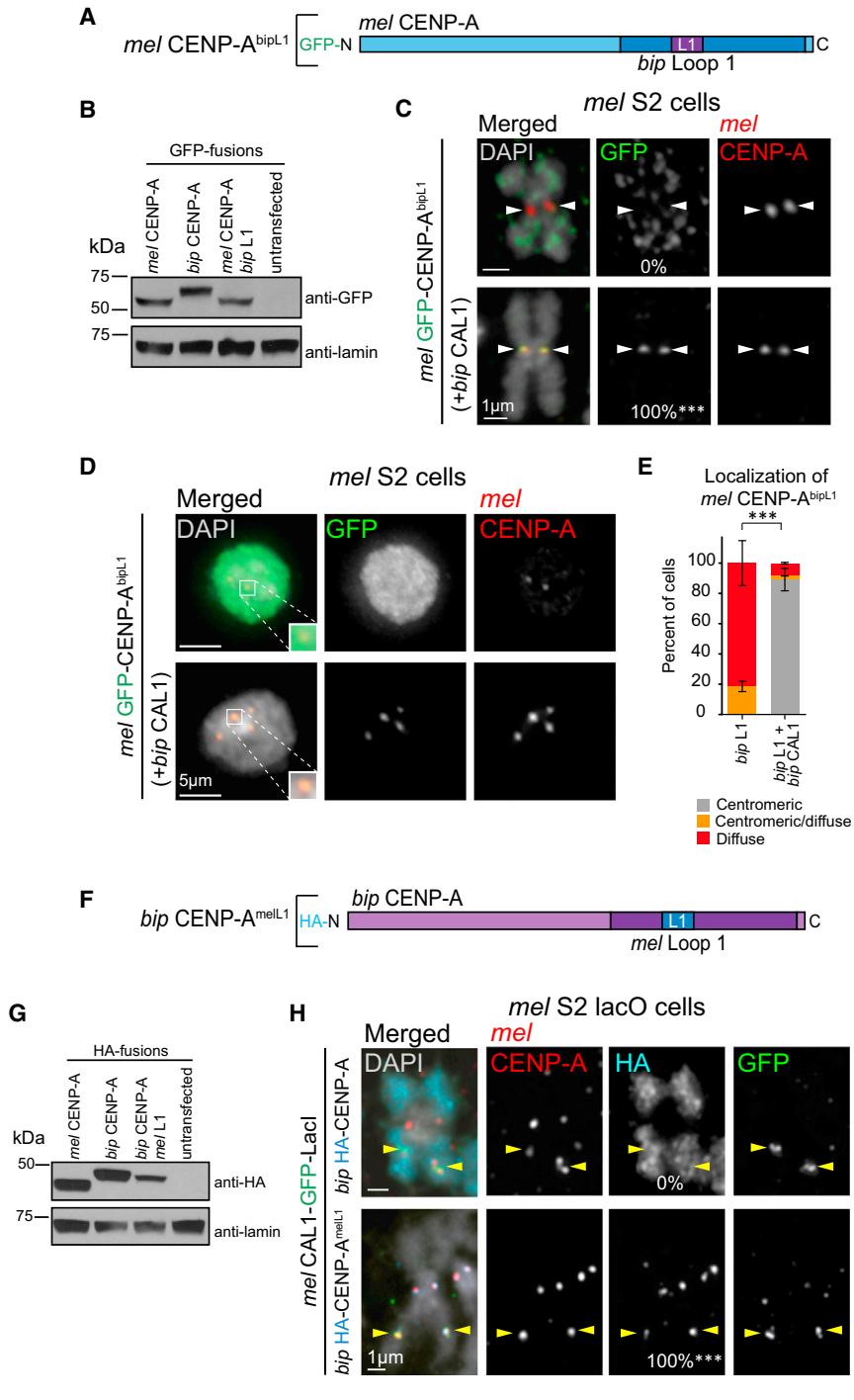

Figure 4. CAL1 Recognizes CENP-A via L1

(A) Schematic of *mel* CENP-A construct with *bip* L1 substituted into the *mel* HFD (*mel* GFP-CENP-A^{bipL1}). Blue represents the *mel* CENP-A protein sequence; *bip* CENP-A amino acids are indicated in purple.

(B) Western blots of whole-cell extracts showing the expression levels and size of GFP-*mel* CENP-A^{bipL1} chimera compared with GFP-*mel* CENP-A and GFP-*bip* CENP-A. Top: anti-GFP; bottom: anti-lamin (loading control).

(C) IF images of metaphase spreads from S2 cells transiently expressing GFP-*mel* CENP-A^{bipL1} chimera alone, or co-expressed with *bip* CAL1. DAPI is shown in gray, GFP in green, and *mel* CENP-A in red. White arrowheads indicate position of the centromere. n = 9 for *mel* CENP-A^{bipL1} chimera alone and n = 10 for *mel* CENP-A^{bipL1} chimera with *bip* CAL1. The percentage of cells with centromeric GFP signal is as indicated in the middle column. ***p < 0.0001; Fisher's two-tailed test of cells with compared with cells without *bip* CAL1. These data were confirmed by two biological replicates (data not shown).

(D) IF images of interphase S2 cells transiently expressing GFP-*mel* CENP-A^{bipL1} chimera alone or co-expressed with *bip* CAL1. DAPI is shown in gray, GFP in green, and *mel* CENP-A in red. Zoomed panels show representative centromeres with merged colors.

(E) Quantification of the IF shown in D. GFP-CENP-A^{bipL1} chimera localization was classified as centromeric (gray bars), diffuse (red), or centromeric and diffuse (orange). n = 70 cells quantified for *mel* CENP-A^{bipL1} chimera and 83 for *mel* CENP-A^{bipL1} chimera with *bip* CAL1. Error bars denote the SD of three biological replicates. ***p < 0.0001; Fisher's two-tailed test comparing cells with and without *bip* CAL1.

(F) Schematic of *bip* CENP-A construct with *mel* L1 substituted into the HFD (*bip* CENP-A^{melL1}; HA-tagged). *mel* CENP-A residues are represented in blue and *bip* CENP-A amino acids in purple. HFDs here and in (A) are shown in darker shades of the respective colors.

(G) Western blots of whole-cell extracts showing the expression levels and of the *bip* HA-CENP-A^{melL1} chimera compared with *mel* HA-CENP-A and *bip* HA-CENP-A. Top: anti-HA; bottom: anti-lamin (loading control).

(H) IF images of metaphase chromosome spreads from *mel* lacO S2 cells transiently expressing *mel* CAL1-GFP-LacI (green) and HA-tagged *bip* CENP-A or *bip* CENP-A^{melL1} chimera (aqua). Endogenous *mel* CENP-A is shown in red, DAPI in gray. Yellow arrowheads indicate the position lacO array. n = 20 for HA-tagged *bip* CENP-A and 16 for HA *bip* CENP-A^{melL1} chimera. The recruitment efficiency to the lacO site for each HA-tagged construct is indicated at the bottom of the HA panel. ***p < 0.0001; Fisher's two-tailed test. These results were confirmed by two biological replicates (data not shown).

regions of *bip* CAL1 that may have adaptively evolved with *bip* CENP-A. Such a region within *bip* CAL1 could confer *mel* CAL1 the ability to deposit *bip* CENP-A if introduced through amino acid swap experiments. Because the CENP-A interaction domain of CAL1 lies within its N terminus (*mel* residues 1–407 [Chen et al., 2014; Schittenhelm et al., 2010]; corresponding to 1–420 in *bip*), we focused on this region to create CAL1 N-terminal *bip-mel* chimeras (Figures 5A and 5B) and interrogated their competency for *bip* CENP-A recruitment at the lacO site.

Residues 1–160 of *mel* CAL1 are sufficient for CENP-A nucleosome assembly in vitro (Chen et al., 2014). Therefore, we created an N-terminal CAL1 (1–407) chimera where the first

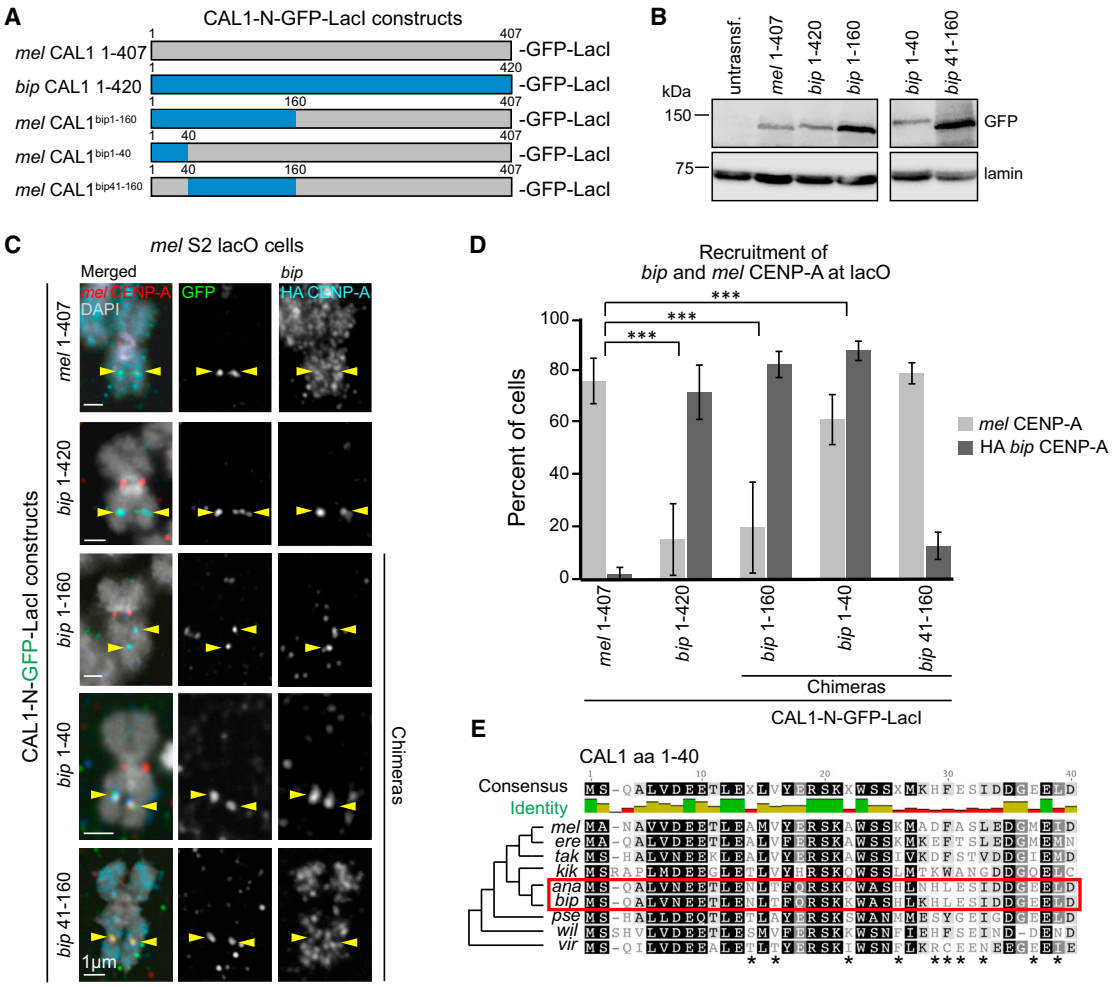

Figure 5. Identification of CAL1 Residues Co-evolving with CENP-A L1

(A) Schematic of N-terminal CAL1-GFP-LacI constructs. For chimeras, gray indicates *mel* CAL1 and blue indicates *bip* CAL1 proteins.

(B) Western blots of whole-cell extracts showing the expression and sizes of the N-CAL1-GFP-LacI constructs used in these experiments (top: anti-GFP; bottom: anti-lamin loading control).

(C) IF images of metaphase chromosome spreads from *mel* lacO S2 cells transiently expressing the indicated N-CAL1-GFP-LacI constructs from (A), along with *bip* HA-CENP-A. GFP is shown in green, HA in aqua, *mel* CENP-A in red, and DAPI in gray. Yellow arrowheads indicate the position of the lacO array. Note that since the N terminus of CAL1 alone cannot localize to centromeres (Chen et al., 2014), these constructs are not expected to deposit *bip* CENP-A at the endogenous centromere.

(D) Quantification of the IF shown in (C). Error bars represent the SD of three biological replicates. n = 160 spreads for *mel* CAL1 1–407, 82 for *bip* CAL1 1–420, 127 for *mel* CAL1$^{bip1-160}$, 127 for *mel* CAL1$^{bip1-40}$, and 91 for *mel* CAL1$^{bip41-160}$. ***$p < 0.0001$ when comparing *mel* 1–407 CAL1 recruitment of *bip* CENP-A with that of *bip* CAL1 1–420, *mel* CAL1$^{bip1-160}$, or *mel* CAL1$^{bip1-40}$ (Fisher's two-tailed test).

(E) BLOSUM80 alignment of residues 1–40 of CAL1 from selected species. Shading indicates percent similarity based on the BLOSUM80 score matrix (Henikoff and Henikoff, 1992). Black, 100% similar; dark gray, 80%–100% similar; light gray, 80%–60% similar; white, less than 60% similar. Stars indicate residues that have diverged in the *ananassae* subgroup (red box) compared with the rest of the *melanogaster* group and thus are candidates for residues co-evolving with CENP-A L1. Consensus sequence is shown above the alignment. Percent identity is shown as a bar graph below the consensus sequence: green indicates highly conserved, gold indicates somewhat conserved, and red indicates unconserved.

160 residues of *mel* CAL1 were replaced by the homologous region of *bip* CAL1 (*mel* CAL1$^{bip1-160}$; Figure 5A) fused to GFP-LacI, and determined whether this construct was able to recruit *bip* CENP-A to the lacO site. After induction of *mel* CAL1$^{bip1-160}$-GFP-LacI in lacO cells co-expressing *bip* HA-CENP-A, IF on metaphase spreads was performed with anti-HA, anti-GFP, and anti-*mel* CENP-A antibodies (Figure 5C). We found that *mel* CAL1$^{bip1-160}$-GFP-LacI successfully recruits *bip* CENP-A to the lacO site (82%) while it recruits *mel* CENP-A inefficiently (20%; Figure 5D). These results indicate that replacing the first 160 residues of *mel* CAL1 with the corresponding region of *bip* CAL1 is sufficient to enable the incorporation of *bip* CENP-A into chromatin and that this region is critical for *mel* CENP-A recruitment. Furthermore, as we previously observed that full-length *bip* CAL1 can recruit *mel* CENP-A to the lacO site in approximately 50% of metaphase spreads (Figure 3I), the

lower percentage of recruitment of *mel* CENP-A by the *mel* CAL1$^{bip1-160}$ chimera observed here suggests that the full-length *bip* CAL1 can engage the endogenous centromere/kinetochore assembly pathway, likely via an interaction between its C terminus and *mel* CENP-C (Chen et al., 2014; Schittenhelm et al., 2010).

CAL1 contains an "Scm3-like" domain at its N terminus (Figure 5E; residues 1–40 [Phansalkar et al., 2012]), which is essential for ectopic CENP-A deposition (Chen et al., 2014). To further narrow down the region of CAL1 required for CENP-A incorporation, we swapped residues 1–40 and 41–160 of *mel* CAL1 with the corresponding region of *bip* CAL1 (*mel* CAL1$^{bip1-40}$-GFP-LacI and *mel* CAL1$^{bip41-160}$-GFP-LacI; Figures 5A and 5B). These chimeras were again transiently expressed in S2 lacO cells along with *bip* HA-CENP-A, followed by IF on metaphase spreads to assess the presence or absence of *bip* HA-CENP-A at the lacO (Figure 5C).

We found that *mel* CAL1$^{bip1-40}$-GFP-LacI successfully recruits both *bip* CENP-A and *mel* CENP-A to the lacO (88% and 61%, respectively). In contrast, *mel* CAL1$^{bip41-160}$-GFP-LacI does not efficiently recruit *bip* CENP-A to the lacO site (13%), but still efficiently recruits *mel* CENP-A (79%; Figure 5D). These results suggest that residues 1–40 of *bip* CAL1 are co-evolving with *bip* CENP-A and that the corresponding *mel* CAL1 residues are responsible for the incompatibility observed between *bip* CENP-A and *mel* centromeres (Figures 1 and 5E) (Vermaak et al., 2002). Furthermore, these findings reveal the conservation of CENP-A recognition mechanisms between the non-homologous CAL1 and Scm3/HJURP chaperones, both of which involve the L1 region of CENP-A (Bassett et al., 2012; Cho and Harrison, 2011).

In summary, L1 of CENP-A is evolving adaptively in *Drosophila* (Malik and Henikoff, 2001) and has diverged in the branch containing the *ananassae* subgroup (Vermaak et al., 2002). The Scm3-like region of CAL1 (Phansalkar et al., 2012), which is critical for CENP-A recruitment (Chen et al., 2014), recognizes CENP-A through its L1 and co-evolves with it, thereby maintaining its ability to deposit CENP-A in this branch of the phylogeny. The presence of a competent CAL1 assembly factor (*bip* CAL1 or a *mel* CAL1$^{bip1-40}$ chimera) in *mel* cells is sufficient to deposit *bip* CENP-A into chromatin (centromeric or otherwise).

DISCUSSION

Our work sheds light on a puzzling observation in centromere biology: that a CENP-A ortholog is unable localize to the centromeres of a relatively close species (Vermaak et al., 2002). What makes this even more surprising is the report that yeast CENP-A/Cse4 can complement CENP-A knockdown in HeLa cells (Wieland et al., 2004) despite billions of years since these two species last shared a common ancestor. Using coIPs and an ectopic tethering system, we show that *mel* CAL1 can form a complex with *bip* CENP-A, but this complex is not competent for *bip* CENP-A deposition. Centromeric targeting of *bip* CENP-A can be restored upon co-expression of a functional CAL1 partner in both *mel* and *sim* cells. Using CENP-A and CAL1 chimeras we demonstrate that for successful CENP-A deposition into chromatin to occur residues 1–40 of CAL1 and CENP-A L1 must be compatible, suggesting that these regions mediate CAL1/CENP-A function.

Given that *Drosophila* CENP-A L1 is under positive selection (Malik and Henikoff, 2001), one might predict that its binding partner, CAL1, is also adaptively evolving to maintain centromere integrity throughout evolution. While we found no evidence of positive selection on CAL1 using standard methods (Phansalkar et al., 2012), the lineage-specific CENP-A/CAL1 compatibility demonstrates that the "Scm3-like" domain of CAL1 is undergoing coordinated protein evolution with CENP-A L1.

Secondary functions of CAL1 may be suppressing its rate of evolution. For example, CAL1 also interacts with the highly conserved FACT complex (Chen et al., 2015) and localizes to the nucleolus (Chen et al., 2012; Lidsky et al., 2013). We hypothesize that the overall CAL1 sequence is under purifying selection (Phansalkar et al., 2012) to preserve its functional interactions with highly conserved partners, while key residues within the N terminus of CAL1 evolve to maintain the functional interaction with CENP-A.

Our experiments focused of the role of L1 in centromere evolution. However, the CENP-A N terminus is also adaptively evolving (Malik et al., 2002). Since our experiments used the full-length *bip* CENP-A gene, they demonstrate that the divergent N-terminal tail of *bip* CENP-A does not hinder the ability of *bip* CENP-A to bind to *mel* centromeres when *bip* CAL1 is present, at least in mitosis, challenging the proposal that the N terminus also evolves in conflict with centromeric DNA. However, we cannot exclude the possibility that the adaptive evolution of the CENP-A N terminus may be a contributing factor in modulating the DNA-binding preferences of CENP-A exclusively during meiosis, as the N terminus of CENP-A has been shown to have meiosis-specific functions in *Arabidopsis* (Lermontova et al., 2006; Ravi and Chan, 2010).

Since we have not directly assayed the CENP-A-associated DNA sequences of any of these *Drosophila* species, we are unable to completely rule out the divergence of centromeric DNA as a contributing factor in the adaptive evolution of CENP-A L1. Nonetheless, *bip* CENP-A can localize to both *mel* and *sim* centromeres, suggesting that the presence of a functionally compatible CENP-A chaperone is what determines the ability of CENP-A orthologs to be incorporated at the centromeres of both species. Even the more divergent *wil* CENP-A can localize to *mel* centromeres in the presence of its CAL1 partner. It is possible that *mel*, *sim*, *bip*, and *wil* all share the same centromeric sequences. However, such divergent species (spanning 40 million years of evolution), having experienced no changes in centromeric DNA sequences, would go against the fundamental assumption of centromere drive that centromeric satellites are rapidly evolving. Collectively, our data are inconsistent with positive selection of CENP-A L1 affecting its DNA-binding preferences throughout evolution (Malik and Henikoff, 2001; Vermaak et al., 2002).

The question of why CENP-A is rapidly evolving in *Drosophila* still remains, and experimental evidence that CENP-A evolution is a direct result of conflict with centromeric DNA is lacking. CAL1 is unlikely to drive this rapid evolution, since it is evolving more slowly than CENP-A (Phansalkar et al., 2012). We propose that, in *Drosophila*, positive selection of CENP-A L1 modulates the efficiency of its centromeric deposition by CAL1 rather than

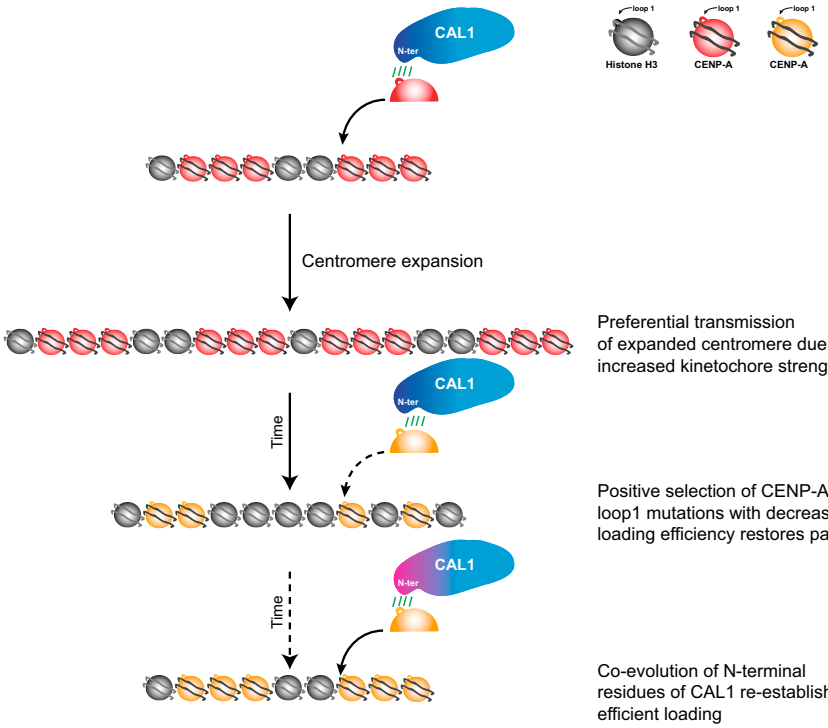

Figure 6. Model for the Co-evolution of CENP-A L1 and CAL1 in the Context of Centromere Drive

CENP-A centromeric deposition by CAL1 requires compatibility between the CAL1 N terminus and L1 (loop 1) of CENP-A. When centromere expansion occurs as a result of unequal crossover during meiosis, the larger and thus stronger centromere will be preferentially transmitted to the next generation (centromere drive) (Henikoff and Malik, 2002; Malik and Henikoff, 2002). To restore meiotic parity, positive selection of L1 mutations (Malik and Henikoff, 2001) weakens the ability of CAL1 to assemble CENP-A into chromatin, resulting in lower levels of CENP-A being deposited. The N terminus of CAL1 co-evolves, albeit at a slower rate, and re-establishes efficient CENP-A deposition, thereby maintaining centromere identity.

its DNA-binding specificity, as originally proposed (Vermaak et al., 2002). Our analysis of the extreme example of the incompatible *bip* CENP-A and *mel* CAL1 suggests that the degree of functional compatibility between these two proteins during intermediate evolutionary times could influence how much CENP-A is incorporated, in turn affecting CENP-C recruitment and kinetochore assembly (Chen et al., 2014; Erhardt et al., 2008). Thus, the ability to "tune" how much CENP-A is deposited at the centromere via changes in L1 could be a mechanism to curb the increased "kinetochore strength" resulting from centromere satellite expansion during centromere drive (Figure 6), akin to the long-standing model proposed by Henikoff and Malik (Henikoff and Malik, 2002; Malik and Henikoff, 2002). Although our work focuses on the critical role of these co-evolving domains in mitosis, it is important to note that CAL1 is also essential for CENP-A deposition during meiosis (Dunleavy et al., 2012). Therefore it is conceivable that our proposed model would apply to meiosis, the natural battleground of centromere drive.

EXPERIMENTAL PROCEDURES

Plasmids

Flies and genomic DNA were obtained from the University of California San Diego Drosophila Species Stock Center or from other laboratories (see Table S1). All non-*melanogaster* CENP-A and CAL1 orthologs were PCR amplified using Phusion High-Fidelity DNA polymerase (New England Biolabs) from genomic DNA using the primers listed in Table S2. See Supplemental Experimental Procedures for details on cloning.

Cell Culture and Transfections

Drosophila melanogaster Schneider 2 (S2) cells were grown as described previously (Chen et al., 2014; Mellone et al., 2011). S2 cells containing stably integrated LacO arrays (pAFS5 [Straight et al., 1996]) were generated as described previously (Chen et al., 2014; Mendiburo et al., 2011). *Drosophila simulans* ML82-19a (M-19) cells were purchased from the Drosophila Genomics Resource Center. M-19 cells were grown in Schneider's media with 10% fetal bovine serum at 25°C.

Transient and stable transfections in S2 cells were performed using FuGENE HD Transfection Reagent (Promega) as previously described (Chen et al., 2014). For transient transfection in M-19 cells, 2×10^6 cells were plated in six-well plates and transfected with Cellfectin reagent (Invitrogen) and plasmid DNA. Cells were incubated with the transfection complex in serum-free medium for 3 hr before replacing medium with serum-containing medium. Cells were incubated for 3 days before harvesting for IF.

Metaphase Chromosome Spreads and IF

IF on settled interphase cells and metaphase spreads were performed as previously described (Chen et al., 2014). Primary antibodies: anti-CENP-A (chicken, 1:1,500; Blower and Karpen, 2001) or anti-CID (rabbit, 1:500; Abcam), anti-CENP-C (guinea pig, 1:500; Erhardt et al., 2008), anti-Ndc80 (chicken, 1:200; Cane et al., 2013), anti-GFP Alexa 488-conjugated (rabbit, 1:100; Invitrogen), or anti-GFP (chicken, 1:500; Abcam), and anti-HA (mouse, 1:500; Covance).

For salt extractions, settled cells were incubated with PBS-D (0.1% digitonin) with or without 0.5 M NaCl for 30 min (Perpelescu et al., 2009) before 37% formaldehyde was added to the solution to a final concentration of 3.7% followed by 10 min of incubation before proceeding with IF.

Imaging

Images were acquired on a wide-field fluorescence microscope (PersonalDV; GE Healthcare) equipped with a 60 Å~/1.42 NA or a 100 Å~/1.40 NA oil-immersion objective (Olympus) and a CoolSnap HQ2 camera (Photometrics), keeping exposure conditions constant between all samples. Images were acquired and processed in softWoRx (Applied Precision), maintaining the scaling constant between samples, and saved as PSD files. Figures were assembled in Adobe Illustrator. For quantification, see Supplemental Experimental Procedures.

Western Blots and IPs

Whole-cell lysates and western blots were prepared as previously described (Chen et al., 2014). Membranes were incubated with either anti-GFP (Goat, 1:150; Rockland), anti-CAL1 (rabbit, 1:000; gift from Aaron Straight), anti-HA (mouse, 1:500; Covance), anti-tubulin (mouse, 1:500; Sigma-Aldrich), anti-fibrillarin (mouse, 1:1,000; Cytoskeleton), or anti-lamin (mouse, 1:1,000; Hybridoma Bank, University of Iowa) primary antibodies. Blots were imaged on an Odyssey Fc (LI-COR Biosciences) using chemiluminescent substrate for detection of horseradish peroxidase-labeled secondary antibodies, or were developed on X-ray films.

IPs were performed from nuclear extracts as previously described (Chen et al., 2012), using 5 μg of anti-CAL1 antibody or 5 μg of anti-immunoglobulin G antibody. For normalization, whole-cell lysates were prepared from 1×10^6 cells expressing either *mel* or *bip* GFP-CENP-A, and total GFP protein levels were quantified by western blotting using Image Studio software (LI-COR) and normalized compared with a loading control (lamin). Nuclear extracts were performed from the same cells and were diluted in resuspension buffer (0.29 M sucrose, 0.5 mM Tris-HCl [pH 7.4], 1.5 mM NaCl, 5 mM $MgCl_2$, 1 mM EGTA, 0.04% Triton X-100, 1× EDTA-free protease inhibitors, and 1 mM DTT) so that the levels of GFP-CENP-A in all samples were equal. 150 μl of diluted *bip* or undiluted *mel* nuclear extract were loaded onto antibody-conjugated beads for IP. See Supplemental Experimental Procedures for quantification of IPs.

SUPPLEMENTAL INFORMATION

Supplemental Information includes Supplemental Experimental Procedures, six figures, and two tables and can be found with this article online at http://dx.doi.org/10.1016/j.devcel.2016.03.021.

AUTHOR CONTRIBUTIONS

B.G.M. and L.R. conceived the project; L.R. conducted experiments; B.G.M. and L.R. wrote the manuscript.

ACKNOWLEDGMENTS

We thank Gary Karpen, Aaron Straight, Patrick Heun, and Tom Maresca for reagents; Rachel O'Neill and Eric Joyce for critically reading the manuscript; Jason Palladino and Chin-Chi Chen for discussions and suggestions; Harmit Malik for fly genomic DNA; Doris Bachtrog, Rich Meisel, and Andy Clark for flies; Patrick Lenehan, Chin-Chi Chen, and Ankita Chavan for technical help; and Flybase, the UCSD Stock Center, and the DGRC for fly stocks and other *Drosophila* resources. L.R. was supported by NSF award MCB1330667; B.G.M. was supported by NSF award MCB1330667 and NIH award GM108829.

Received: November 30, 2015
Revised: March 4, 2016
Accepted: March 22, 2016
Published: April 18, 2016

REFERENCES

Bassett, E.A., DeNizio, J., Barnhart-Dailey, M.C., Panchenko, T., Sekulic, N., Rogers, D.J., Foltz, D.R., and Black, B.E. (2012). HJURP uses distinct CENP-A surfaces to recognize and to stabilize CENP-A/histone H4 for centromere assembly. Dev. Cell *22*, 749–762.

Bernad, R., Sánchez, P., Rivera, T., Rodríguez-Corsino, M., Boyarchuk, E., Vassias, I., Ray-Gallet, D., Arnaoutov, A., Dasso, M., Almouzni, G., et al. (2011). *Xenopus* HJURP and condensin II are required for CENP-A assembly. J. Cell Biol. *192*, 569–582.

Black, B.E., Foltz, D.R., Chakravarthy, S., Luger, K., Woods, V.L., and Cleveland, D.W. (2004). Structural determinants for generating centromeric chromatin. Nature *430*, 578–582.

Blower, M.D., and Karpen, G.H. (2001). The role of Drosophila CID in kinetochore formation, cell-cycle progression and heterochromatin interactions. Nat. Cell Biol. *3*, 730–739.

Camahort, R., Li, B., Florens, L., Swanson, S.K., Washburn, M.P., and Gerton, J.L. (2007). Scm3 is essential to recruit the histone H3 variant Cse4 to centromeres and to maintain a functional kinetochore. Mol. Cell *26*, 853–865.

Cane, S., Ye, A.A., Luks-Morgan, S.J., and Maresca, T.J. (2013). Elevated polar ejection forces stabilize kinetochore-microtubule attachments. J. Cell Biol. *200*, 203–218.

Chen, C.-C., Greene, E., Bowers, S.R., and Mellone, B.G. (2012). A role for the CAL1-partner Modulo in centromere integrity and accurate chromosome segregation in *Drosophila*. PLoS One *7*, e45094.

Chen, C.-C., Dechassa, M.L., Bettini, E., Ledoux, M.B., Belisario, C., Heun, P., Luger, K., and Mellone, B.G. (2014). CAL1 is the *Drosophila* CENP-A assembly factor. J. Cell Biol. *204*, 313–329.

Chen, C.-C., Bowers, S., Lipinszki, Z., Palladino, J., Trusiak, S., Bettini, E., Rosin, L., Przewloka, M.R., Glover, D.M., O'Neill, R.J., et al. (2015). Establishment of centromeric chromatin by the CENP-A assembly factor CAL1 requires FACT-mediated transcription. Dev. Cell *34*, 73–84.

Chmátal, L., Gabriel, S.I., Mitsainas, G.P., Martínez-Vargas, J., Ventura, J., Searle, J.B., Schultz, R.M., and Lampson, M.A. (2014). Centromere strength provides the cell biological basis for meiotic drive and karyotype evolution in mice. Curr. Biol. *24*, 2295–2300.

Cho, U.-S., and Harrison, S.C. (2011). Recognition of the centromere-specific histone Cse4 by the chaperone Scm3. Proc. Natl. Acad. Sci. USA *108*, 9367–9371.

Choo, K.H. (2000). Centromerization. Trends Cell Biol. *10*, 182–188.

Cooper, J.L., and Henikoff, S. (2004). Adaptive evolution of the histone fold domain in centromeric histones. Mol. Biol. Evol. *21*, 1712–1718.

Daniel, A. (2002). Distortion of female meiotic segregation and reduced male fertility in human Robertsonian translocations: consistent with the centromere model of co-evolving centromere DNA/centromeric histone (CENP-A). Am. J. Med. Genet. *111*, 450–452.

Dunleavy, E.M., Roche, D., Tagami, H., Lacoste, N., Ray-Gallet, D., Nakamura, Y., Daigo, Y., Nakatani, Y., and Almouzni-Pettinotti, G. (2009). HJURP is a cell-cycle-dependent maintenance and deposition factor of CENP-A at centromeres. Cell *137*, 485–497.

Dunleavy, E.M., Beier, N.L., Gorgescu, W., Tang, J., Costes, S.V., and Karpen, G.H. (2012). The cell cycle timing of centromeric chromatin assembly in *Drosophila* meiosis is distinct from mitosis yet requires CAL1 and CENP-C. PLoS Biol. *10*, e1001460.

Earnshaw, W.C., and Rothfield, N. (1985). Identification of a family of human centromere proteins using autoimmune sera from patients with scleroderma. Chromosoma *91*, 313–321.

Erhardt, S., Mellone, B.G., Betts, C.M., Zhang, W., Karpen, G.H., and Straight, A.F. (2008). Genome-wide analysis reveals a cell cycle-dependent mechanism controlling centromere propagation. J. Cell Biol. *183*, 805–818.

Finseth, F.R., Dong, Y., Saunders, A., and Fishman, L. (2015). Duplication and adaptive evolution of a key centromeric protein in mimulus, a genus with female meiotic drive. Mol. Biol. Evol. *32*, 2694–2706.

Fishman, L., and Saunders, A. (2008). Centromere-associated female meiotic drive entails male fitness costs in monkeyflowers. Science *322*, 1559–1562.

Fishman, L., and Willis, J.H. (2005). A novel meiotic drive locus almost completely distorts segregation in mimulus (monkeyflower) hybrids. Genetics *169*, 347–353.

Foltz, D.R., Jansen, L.E.T., Bailey, A.O., Yates, J.R., 3rd, Bassett, E.A., Wood, S., Black, B.E., and Cleveland, D.W. (2009). Centromere-specific assembly of CENP-A nucleosomes is mediated by HJURP. Cell *137*, 472–484.

Fukagawa, T., and Earnshaw, W.C. (2014). The centromere: chromatin foundation for the kinetochore machinery. Dev. Cell *30*, 496–508.

Henikoff, S., and Henikoff, J.G. (1992). Amino acid substitution matrices from protein blocks. Proc. Natl. Acad. Sci. USA *89*, 10915–10919.

Henikoff, S., and Malik, H.S. (2002). Centromeres: selfish drivers. Nature *417*, 227.

Henikoff, S., Ahmad, K., and Malik, H.S. (2001). The centromere paradox: stable inheritance with rapidly evolving DNA. Science *293*, 1098–1102.

Heun, P., Erhardt, S., Blower, M.D., Weiss, S., Skora, A.D., and Karpen, G.H. (2006). Mislocalization of the *Drosophila* centromere-specific histone CID promotes formation of functional ectopic kinetochores. Dev. Cell *10*, 303–315.

Karpen, G.H., and Allshire, R.C. (1997). The case for epigenetic effects on centromere identity and function. Trends Genet. *13*, 489–496.

Lermontova, I., Schubert, V., Fuchs, J., Klatte, S., Macas, J., and Schubert, I. (2006). Loading of Arabidopsis centromeric histone CENH3 occurs mainly during G2 and requires the presence of the histone fold domain. Plant Cell *18*, 2443–2451.

Lidsky, P.V., Sprenger, F., and Lehner, C.F. (2013). Distinct modes of centromere protein dynamics during cell cycle progression in *Drosophila* S2R+ cells. J. Cell Sci. *126*, 4782–4793.

Luger, K., Mäder, A.W., Richmond, R.K., Sargent, D.F., and Richmond, T.J. (1997). Crystal structure of the nucleosome core particle at 2.8 A resolution. Nature *389*, 251–260.

Malik, H.S. (2009). The centromere-drive hypothesis: a simple basis for centromere complexity. Prog. Mol. Subcell. Biol. *48*, 33–52.

Malik, H.S., and Henikoff, S. (2001). Adaptive evolution of Cid, a centromere-specific histone in *Drosophila*. Genetics *157*, 1293–1298.

Malik, H.S., and Henikoff, S. (2002). Conflict begets complexity: the evolution of centromeres. Curr. Opin. Genet. Dev. *12*, 711–718.

Malik, H.S., Vermaak, D., and Henikoff, S. (2002). Recurrent evolution of DNA-binding motifs in the *Drosophila* centromeric histone. Proc. Natl. Acad. Sci. USA *99*, 1449–1454.

Mellone, B.G., Grive, K.J., Shteyn, V., Bowers, S.R., Oderberg, I., and Karpen, G.H. (2011). Assembly of *Drosophila* centromeric chromatin proteins during mitosis. PLoS Genet. *7*, e1002068.

Melters, D.P., Bradnam, K.R., Young, H.A., Telis, N., May, M.R., Ruby, J.G., Sebra, R., Peluso, P., Eid, J., Rank, D., et al. (2013). Comparative analysis of tandem repeats from hundreds of species reveals unique insights into centromere evolution. Genome Biol. *14*, R10.

Mendiburo, M.J., Padeken, J., Fülöp, S., Schepers, A., and Heun, P. (2011). *Drosophila* CENH3 is sufficient for centromere formation. Science *334*, 686–690.

Meraldi, P., McAinsh, A.D., Rheinbay, E., and Sorger, P.K. (2006). Phylogenetic and structural analysis of centromeric DNA and kinetochore proteins. Genome Biol. *7*, R23.

Mizuguchi, G., Xiao, H., Wisniewski, J., Smith, M.M., and Wu, C. (2007). Nonhistone Scm3 and histones CenH3-H4 assemble the core of centromere-specific nucleosomes. Cell *129*, 1153–1164.

Moreno-Moreno, O., Medina-Giró, S., Torras-Llort, M., and Azorín, F. (2011). The F box protein partner of paired regulates stability of *Drosophila* centromeric histone H3, CenH3CID. Curr. Biol. *21*, 1488–1493.

Olszak, A.M., van Essen, D., Pereira, A.J., Diehl, S., Manke, T., Maiato, H., Saccani, S., and Heun, P. (2011). Heterochromatin boundaries are hotspots for de novo kinetochore formation. Nat. Cell Biol. *13*, 799–808.

Pardo-Manuel de Villena, F., and Sapienza, C. (2001). Female meiosis drives karyotypic evolution in mammals. Genetics *159*, 1179–1189.

Perpelescu, M., Nozaki, N., Obuse, C., Yang, H., and Yoda, K. (2009). Active establishment of centromeric CENP-A chromatin by RSF complex. J. Cell Biol. *185*, 397–407.

Phansalkar, R., Lapierre, P., and Mellone, B.G. (2012). Evolutionary insights into the role of the essential centromere protein CAL1 in *Drosophila*. Chromosome Res. *20*, 493–504.

Pidoux, A.L., Choi, E.S., Abbott, J.K.R., Liu, X., Kagansky, A., Castillo, A.G., Hamilton, G.L., Richardson, W., Rappsilber, J., He, X., et al. (2009). Fission yeast Scm3: a CENP-A receptor required for integrity of subkinetochore chromatin. Mol. Cell *33*, 299–311.

Ravi, M., and Chan, S.W.L. (2010). Haploid plants produced by centromere-mediated genome elimination. Nature *464*, 615–618.

Ravi, M., Kwong, P.N., Menorca, R.M.G., Valencia, J.T., Ramahi, J.S., Stewart, J.L., Tran, R.K., Sundaresan, V., Comai, L., and Chan, S.W.-L. (2010). The rapidly evolving centromere-specific histone has stringent functional requirements in *Arabidopsis thaliana*. Genetics *186*, 461–471.

Sanchez-Pulido, L., Pidoux, A.L., Ponting, C.P., and Allshire, R.C. (2009). Common ancestry of the CENP-A chaperones Scm3 and HJURP. Cell *137*, 1173–1174.

Schittenhelm, R.B., Althoff, F., Heidmann, S., and Lehner, C.F. (2010). Detrimental incorporation of excess Cenp-A/Cid and Cenp-C into *Drosophila* centromeres is prevented by limiting amounts of the bridging factor Cal1. J. Cell Sci. *123*, 3768–3779.

Schueler, M.G., Swanson, W., Thomas, P.J., Comparative Sequencing Program, N.I.S.C., and Green, E.D. (2010). Adaptive evolution of foundation kinetochore proteins in primates. Mol. Biol. Evol. *27*, 1585–1597.

Sekulic, N., Bassett, E.A., Rogers, D.J., and Black, B.E. (2010). The structure of (CENP-A-H4)2 reveals physical features that mark centromeres. Nature *467*, 347–351.

Shelby, R.D., Vafa, O., and Sullivan, K.F. (1997). Assembly of CENP-A into centromeric chromatin requires a cooperative array of nucleosomal DNA contact sites. J. Cell Biol. *136*, 501–513.

Straight, A.F., Belmont, A.S., Robinett, C.C., and Murray, A.W. (1996). GFP tagging of budding yeast chromosomes reveals that protein–protein interactions can mediate sister chromatid cohesion. Curr. Biol. *6*, 1599–1608.

Tachiwana, H., Kagawa, W., and Kurumizaka, H. (2012). Comparison between the CENP-A and histone H3 structures in nucleosomes. Nucl. Austin Tex. *3*, 6–11.

Talbert, P.B., Masuelli, R., Tyagi, A.P., Comai, L., and Henikoff, S. (2002). Centromeric localization and adaptive evolution of an *Arabidopsis* histone H3 variant. Plant Cell *14*, 1053–1066.

Vermaak, D., Hayden, H.S., and Henikoff, S. (2002). Centromere targeting element within the histone fold domain of CID. Mol. Cell Biol. *22*, 7553–7561.

Wieland, G., Orthaus, S., Ohndorf, S., Diekmann, S., and Hemmerich, P. (2004). Functional complementation of human centromere protein A (CENP-A) by Cse4p from Saccharomyces cerevisiae. Mol. Cell Biol. *24*, 6620–6630.

Wyttenbach, A., Borodin, P., and Hausser, J. (1998). Meiotic drive favors Robertsonian metacentric chromosomes in the common shrew (*Sorex araneus*, Insectivora, mammalia). Cytogenet. Cell Genet. *83*, 199–206.

Zedek, F., and Bureš, P. (2012). Evidence for centromere drive in the holocentric chromosomes of *Caenorhabditis*. PLoS One *7*, e30496.

Developmental Cell, Volume *37*

Supplemental Information

Co-evolving CENP-A and CAL1 Domains Mediate Centromeric CENP-A Deposition across *Drosophila* Species

Leah Rosin and Barbara G. Mellone

Supplemental Information

Supplemental Figures and Table Legends

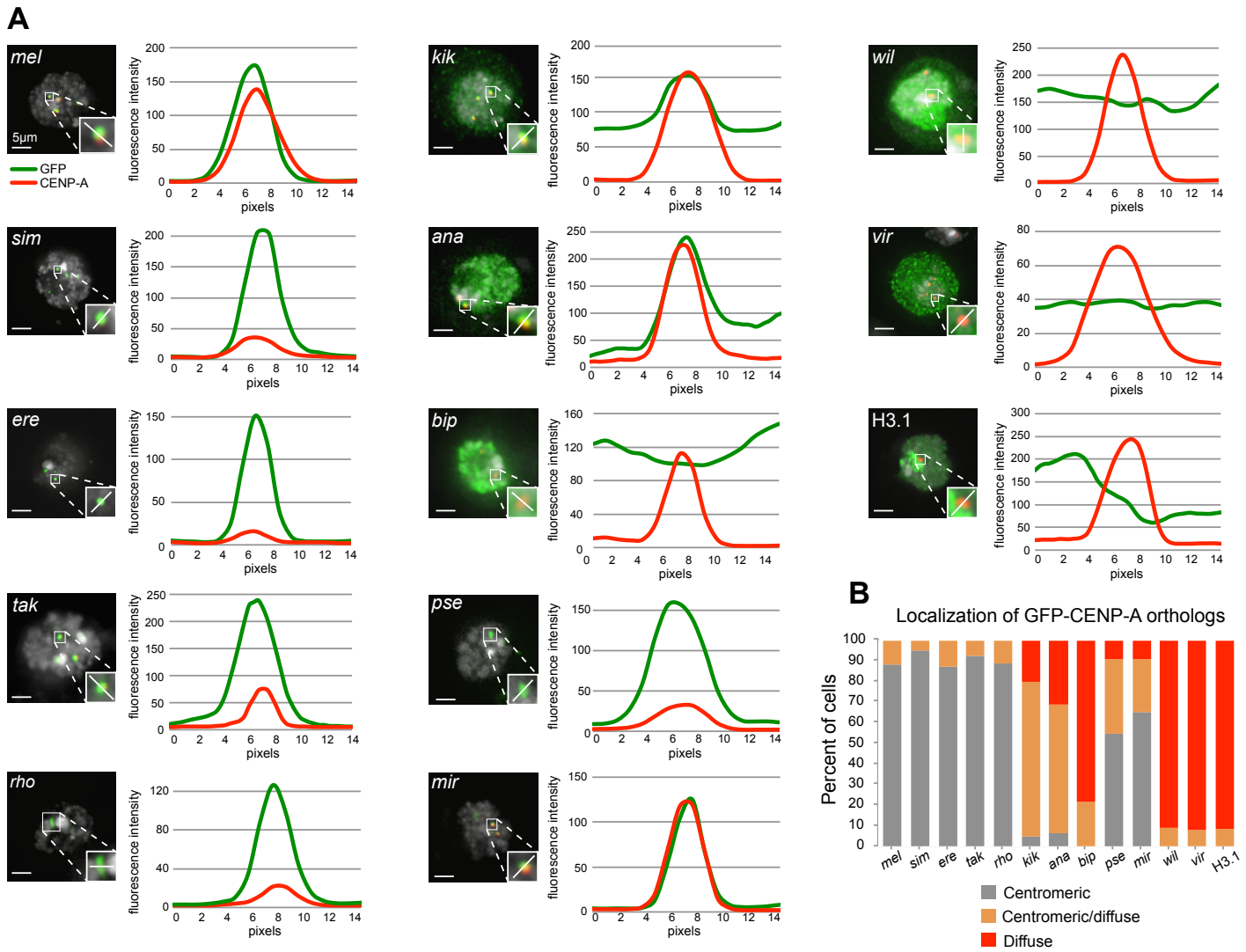

Figure S1, related to Figure 1. Line plots of GFP-tagged CENP-A orthologs and D. *melanogaster* CENP-A localization.
A) Representative IF images of interphase *mel* S2 cells transiently expressing GFP-tagged CENP-A orthologs from the indicated species and corresponding line plots showing the relative CENP-A (red) and GFP (green) fluorescence intensities. DAPI is shown in gray. GFP-H3.1 is shown as a control. B) Quantification of line plots in A. Plots with clear GFP peaks overlapping with *mel* CENP-A peaks and low non-centromeric GFP signal (as in the examples for *mel, sim, ere, tak, rho, pse*) were scored as centromeric (gray bars). Plots displaying both GFP peaks as well as non-centromeric GFP signal (see *kik* and *ana*) were scored as centromeric/diffuse (orange bars), while plots showing no clear GFP peak overlapping with *mel* CENP-A (see as *bip, wil, vir, mel* H3.1) were scored as diffuse (red bars).

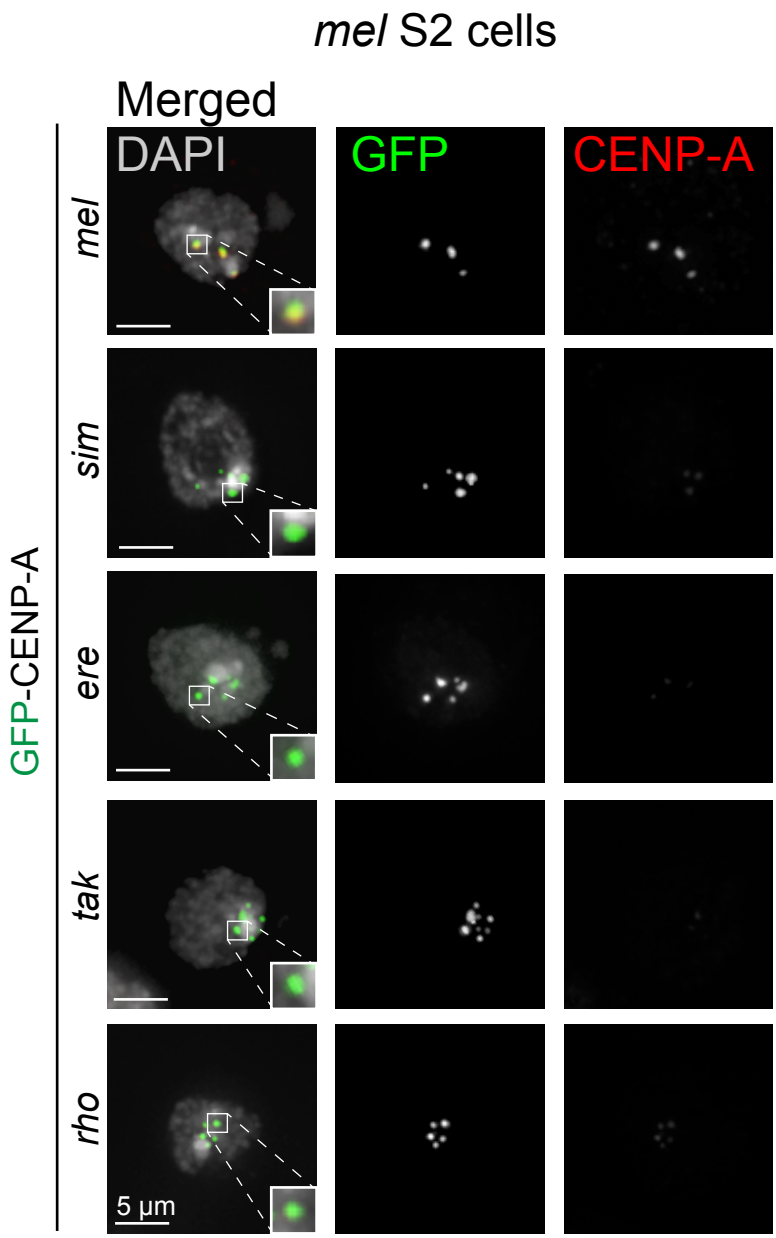

Figure S2, related to Figure 1. Centromeric localization of CENP-A orthologs results in decreased levels of *D. melanogaster* CENP-A in a subset of S2 cells.
IF images of interphase *mel* S2 cells transiently expressing GFP-tagged CENP-A orthologs from *mel*, *sim*, *ere*, *tak*, and *rho* in which endogenous CENP-A levels are noticeably low. Note that the *mel* CENP-A antibody (red) does not recognize CENP-A orthologs from *sim*, *ere*, *tak*, and *rho*. DAPI is shown in grey, GFP in green. Insets show magnified individual centromeres with merged colors.

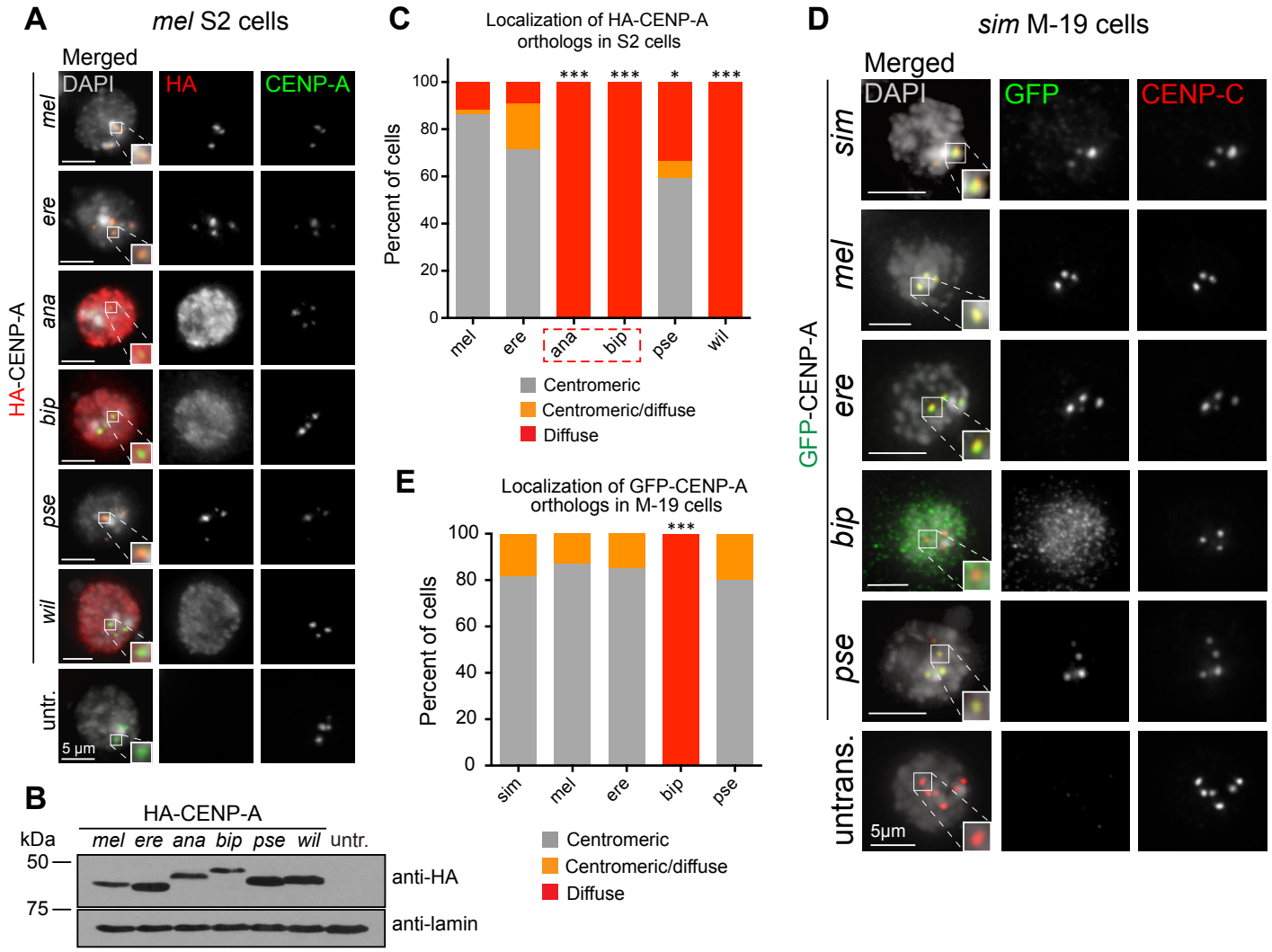

Figure S3, related to Figure 1. *D. bipectinata* CENP-A does not localize to the centromeres of *D. melanogaster* or *D. simulans* cells.

A) Representative IF images of interphase *mel* S2 cells transiently expressing HA-tagged CENP-A orthologs from *mel*, *ere*, *ana*, *bip*, *pse*, and *wil*. DAPI is shown in grey, HA in red, and *mel* CENP-A in green. Zoomed panels show individual centromeres with merged colors.

B) Western blots of total cell extracts showing the expression levels and protein sizes of HA-tagged CENP-A orthologs analyzed in A and B. Lamin antibody (loading control).

C) Quantification of the images shown in A. Images were manually classified as having either centromeric HA signal only (grey bars), diffuse HA signal (red bars), or centromeric and diffuse HA signal (orange bars). n = 50 transfected cells per condition on average. ***p<0.0001 for *ana* or *bip* CENP-A compared to *mel* CENP-A centromeric localization (Fisher's two-tailed test); *p=0.002 for *pse* CENP-A compared to *mel* CENP-A localization (Fisher's two-tailed test). These data were confirmed by one biological replicate with the HA-tag (data not shown) and two with the GFP-tagged constructs (Figure 1).

D) Representative IF images of *sim* M-19 cells transiently expressing GFP-tagged CENP-A orthologs from *mel, sim, ere, bip,* and *pse*. DAPI is shown in grey, GFP in green, and *sim* CENP-C in red. As our CENP-A antibody does not recognize *sim* CENP-A, the CENP-C antibody is used here to mark the native centromere locus. Zoomed panels show individual centromeres with merged colors.

E) Quantification of the images shown in D. Cells were manually classified as having either only centromeric GFP signal (grey bars), diffuse GFP signal (red bars), or centromeric and diffuse (orange

bars). n≥20 cells per condition. These results were confirmed by two biological replicates (data not shown). ***p<0.0001 for *bip* CENP-A compared to *sim* CENP-A centromeric localization (Fisher's two-tailed test).

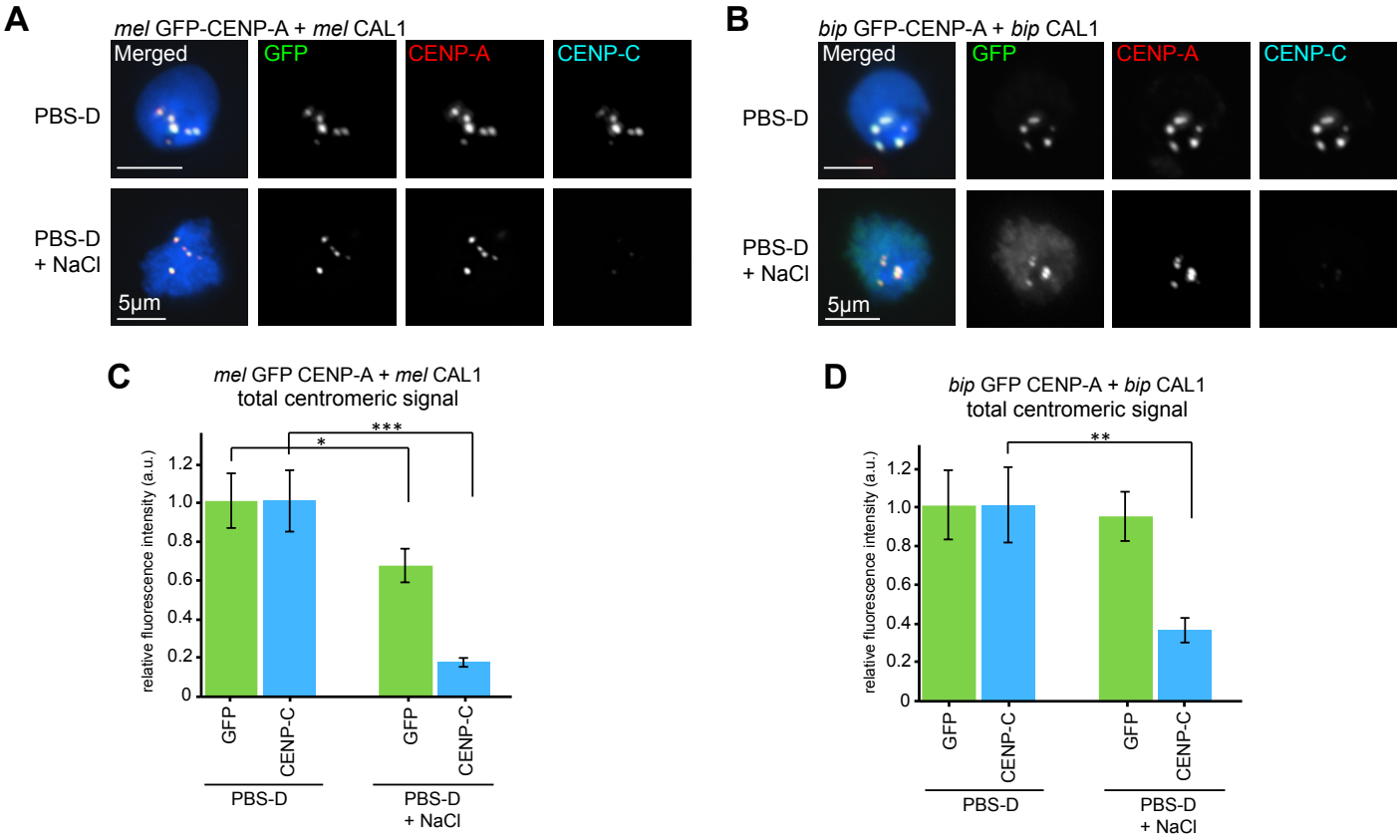

Figure S4, related to Figure 3. Centromere-localized *D. bipectinata* CENP-A is incorporated into chromatin.
A-B) Representative IF images of interphase *mel* S2 cells transiently co-expressing *mel* (A) or *bip* (B) GFP-CENP-A orthologs (green) and *mel* (A) or *bip* (B) HA-CAL1 (not shown). Cells were incubated with PBS-D (0.1% digitonin) plus or minus NaCl prior to fixation. CENP-C is expected to be extracted in the presence of NaCl and is used as a control (Perpelescu et al., 2009). The persistence of signal for GFP-CENP-A orthologs is indicative of chromatin incorporation. DAPI is shown in blue, *mel* CENP-A in red, and *mel* CENP-C in aqua.
C and D) Quantification of IF in A (C) and B (D). The relative fluorescence intensities of GFP CENP-A and CENP-C with and without NaCl incubation are shown. The error bars represent the standard error for an average of n=50 cells per condition. ***p<0.0001, **p=0.002, *p=0.019; unpaired t-test. This experiment was repeated with one biological replicate using PBS-T (0.1% triton) plus or minus NaCl (data not shown).

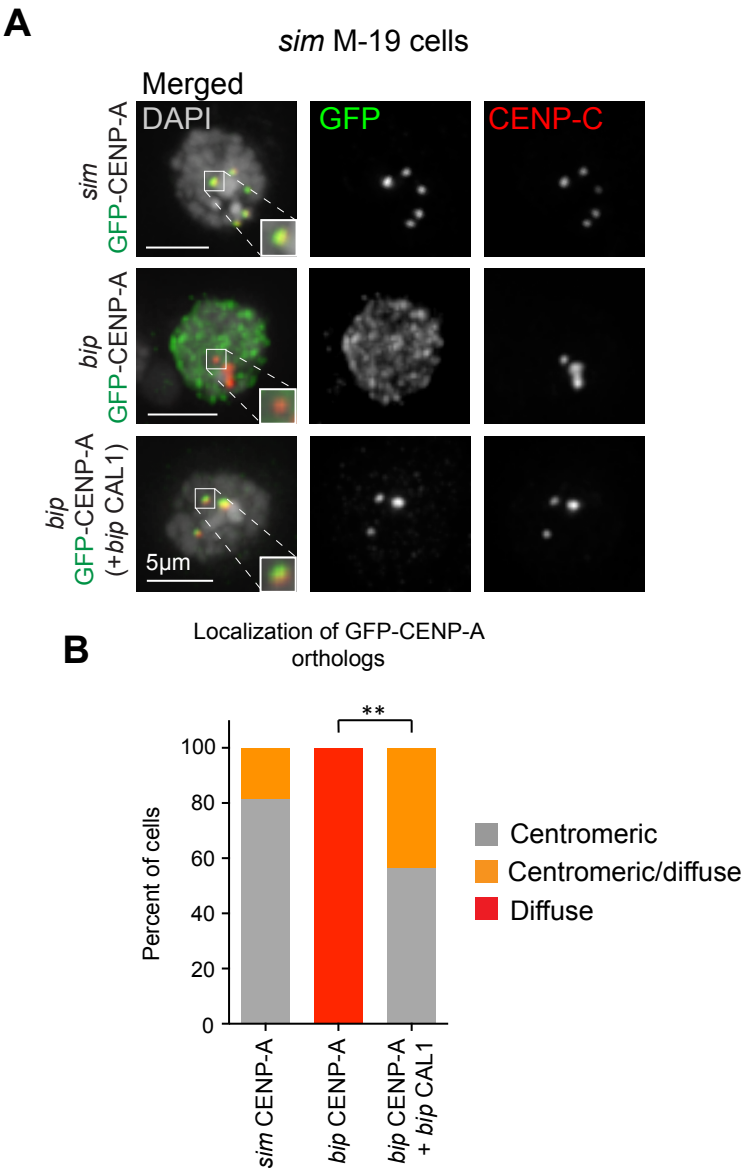

Figure S5, related to Figure 3. *D. bipectinata* CENP-A can localize to *D. simulans* centromeres when co-expressed with *D. bipectinata* CAL1.
A) Representative IF images of interphase *sim* M-19 cells transiently expressing *sim* or *bip* GFP-CENP-A alone (first and second rows, respectively), or *bip* GFP-CENP-A and *bip* HA-CAL1 (third row). DAPI is shown in grey, GFP in green, and CENP-C in red. Zoomed panels show individual centromeres with merged colors.
B) Quantification of the images shown in A. Cells were manually classified as having either exclusively centromeric GFP signal (grey bars), diffuse GFP signal (red bars), or centromeric and diffuse GFP signal (orange bars). n≥30 cells per condition. These data were confirmed by one biological replicate. **p=0.0002 (Fisher's two-tailed test) for the centromeric localization of *bip* CENP-A with and without *bip* CAL1 (data not shown).

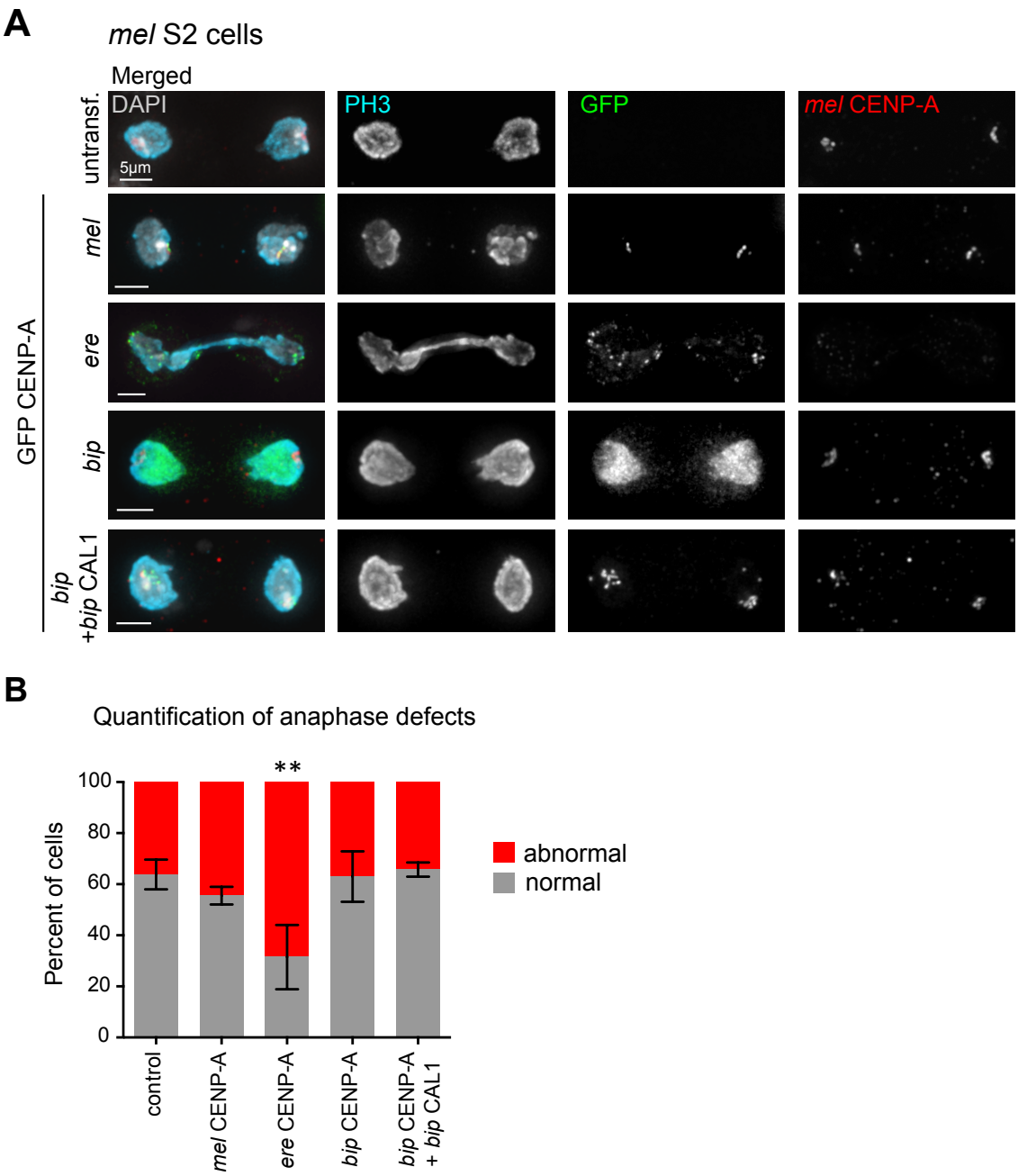

Figure S6, related to Figure 3. The *D. bipectinata* CENP-A/CAL1 complex is sufficient to nucleate *D. melanogaster* kinetochore formation

A) IF images of anaphase S2 cells transiently expressing GFP-CENP-A from *mel*, *ere*, or *bip* (second, third, and fourth column, respectively), or *bip* GFP-CENP-A and *bip* HA-CAL1 (fifth column). The first column shows untransfected S2 cells (GFP-negative). DAPI is shown in grey, GFP in green, *mel* CENP-A in red, and phosphorylated H3S10 (mitotic marker) in aqua.

B) Quantification of the images shown in B. Cells were manually classified as displaying normal (grey) or abnormal (stretched or lagging chromosomes; red) anaphases. The graph shows the average of three biological replicates, and the error bars are the standard deviation of the three biological replicates. n=131 cells total for untransfected images, n=157 for *mel* CENP-A, n=162 for *ere* CENP-A, n=76 for *bip* CENP-A, and n=90 for *bip* CENP-A with *bip* CAL1. **p=0.0009 (Fisher's two-tailed test of cells expressing *ere* CENP-A compared to cells expressing *mel* CENP-A.

Table S1, related to Experimental Procedures. Sources of genomic DNA used for PCR-cloning of *CENP-A* and *CAL1* orthologs.

Drosophila simulans	gDNA from Harmit Malik
Drosophila simulans	Tissue culture cells from DGRC, ML82-19a
Drosophila erecta	gDNA from Harmit Malik
Drosophila takahashii	Flies from UCSD Stock center, #14022-0311.13
Drosophila rhopaloa	Flies from UCSD Stock center, #14029-0021.01
Drosophila kikkawai	Flies from UCSD Stock center, #14028-0561.14
Drosophila ananassae	gDNA from Harmit Malik
Drosophila bipectinata	gDNA from Harmit Malik
Drosophila pseudoobscura	gDNA from Harmit Malik
Drosophila miranda	Flies from Doris Bachtrog
Drosophila wilistoni	Flies from Andy Clark
Drosophila virilis	Flies from Andy Clark

Table S2, related to Experimental Procedures. Primers used for cloning CENP-A and CAL1 orthologs, as well as the *mel* CENP-A^{bipL1} chimera.

mel_CENPA_ascI F	CAAAGGCGCGCCATGCCACGACACAGC
mel_CENPA_pacI R	CGGGTTAATTAACTAAAATTGCCGACCC
pse_CENPA_ascI_F	CAGTGGCGCGCCATGCGACCACCGACAAAAAACAG
pse_CENPA_pacI_R	CAGTTTAATTAATTAGTTAAAGCGACCATGGCTG
ere_CENPA_ascI_F	CAGTGGCGCGCCATGCCCCGACACAATGCTG
ere_CENPA_pacI_R	CAGTTTAATTAACTAGGCCAGCCGACCC
sim_CENPA_ascI_F	CAGTGGCGCGCCATGCCACGACACAGTAGAGCC
sim_CENPA_pacI_R	CAGTTTAATTAACTAAGCTTGCCGACCCCG
ana_CENPA_ascI_F	CAGTGGCGCGCCATGAGACCCCCACCAAAGC
ana_CENPA_pacI_R	CAGTTTAATTAATTAATTACGCCTCAAGTTGTCGC
vir_CENPA_ascI_F	CAGTGGCGCGCCATGCGTCCACGCACTG
vir_CENPA_pacI_R	CAGTTTAATTAATCAAAGATTACCATAGGTTTTGC
bip_CENPA_ascI_F	CAGTGGCGCGCCATGCGACCCCCACCAAAG
bip_CENPA_pacI_R	CAGTTTAATTAACTAGTTCGTCGCAAGGTTCTC
wil_CENPA_ascI_F	CAGTGGCGCGCCATGAGACCCCCTAGAGG
wil_CENPA_pacI_R	CAGTTTAATTAATCAATAGGCACTATCTTTGC
kik_CENPA_ascI_F	GAAAGGCGCGCCATGCGACCACCG
kik_CENPA_pacI_R	CGGGTTAATTAACTAGAGAAGACGATTATGAC
tak_CENPA_ascI_F	GAAAGGCGCGCCATGCCGAGAAAAAGTG
tak_CENPA_pacI_R	CGGGTTAATTAACTAGTTGTGACCCCGG
rho_CENPA_ascI_F	GAAAGGCGCGCCATGCCGAGGCAAG
rho_CENPA_pacI_R	CGGGTTAATTAACTAGAAATGACCCCGG
mir_CENPA_ascI_F	GAAAGGCGCGCCATGCGACCACCG
mir_CENPA_pacI_R	CGGGTTAATTAATTAGTTATATCGACAATGGC

ere_CAL1_ascI_F	CAGTGGCGCGCCATGGCGCAGGCGTT
ere_CAL1_pacI_R	CAGTTTAATTAATCAGTTGTCACCGGAATTATTC
bip_CAL1_ascI_F	CAGTGGCGCGCCATGTCTCAGGCACTGG
bip_CAL1_pacI_R	CAGTTTAATTAACTAGTTCTTCTCCAGAACAC
wil_CAL1_ascI_F	GAAAGGCGCGCCATGTCGTCGCACGTC
wil_CAL1_pacI_R	CGGGTTAATTAATTAGTTGTTTTTATTAGGCTT
pse_CAL1_ascI_F	CAGTGGCGCGCCATGTCGCATGCACTATTGG
pse_CAL1_pacI_R	CAGTTTAATTAATCAATCGTCTGTGGGATC
ere_CAL1_speI_F	CAGTACTAGTATGGCGCAGGCGTTGG
ere_CAL1_notI_R	ATTAGCGGCCGCGGTTGTCACCGGAATTATT
pse_CAL1_speI_F	CAGTACTAGTATGTCGCATGCACTATTGG
pse_CAL1_notI_R	ATTAGCGGCCGCTATCGTCTGTGGGATCC
bip_CAL1_speI_F	CAGTACTAGTATGTCTCAGGCACTGG
bip_CAL1_notI_R	ATTAGCGGCCGCGGTTCTTCTCCAGAACAC
bip_CAL1N_notI_R	CTTGGGCGGCCGCTACAGCCACTAGCTTG
bip_CAL1_XmaI_R	CAGTCCCGGGGTTCTTCTCCAGAACACTG
ana_CAL1_spe1_F	CAGTACTAGTATGTCGCAAGCACTGG
ana_CAL1_notI_R	ATTAGCGGCCGCGGTCCTTCTCCAGTACAC
wil_CAL1_speI_F	CGGGACTAGTATGTCGTCGCACGTCT
wil_CAL1_notI_R	ATTAGCGGCCGCaGTTGTTTTTATTAGGCTTCTCC
wil_CAL1_XmaI_R	CAGTCCCGGGGGTTGTTTTTATTAGGCTTCTC
CENPAmelL1Bip_F2n	CGTCTAGTGCGCGAGCTGCTTTACTCGCAAG
CENPAmelL1Bip_R1n	CTTGCGAGTAAAGCAGCTCGCGCACTAGACG
CENPAmelL1Bip_F3C	GTTCAAAATCTCCACCGGCGCCCTATTGGCC
CENPAmelL1Bip_R2c	GGCCAATAGGGCGCCGGTGGAGATTTTGAAC

Supplemental Experimental Procedures

Plasmids and Cloning

GFP-CENP-A constructs were generated by replacing *mel* CENP-A from the pCopia-LAP-CENP-A vector (Erhardt et al., 2008) with the PCR amplified CENP-A orthologs using AscI and PacI sites (New England Biolabs, Inc.). pCopia-flag-HA constructs were generated in the same way, using the pCopia-HA-CENP-A plasmid (Chen et al., 2014), and replacing *mel* CENP-A with either CENP-A or CAL1 orthologs using AscI and PacI sites. pMT-CAL1-GFP-LacI constructs were generated by replacing CENP-A from the pMT-CENP-A-GFP-LacI construct (Mendiburo et al., 2011) as previously described (Chen et al., 2014, 2015).

The *mel* CENP-A^{bipL1} chimera was created by sequential PCRs followed by cloning using the following primers (see Table S2 for sequences): mel_CENPA_AscI F, CENPAmelL1bip_F2n, CENPAmelL1bip_R1n, CENPAmelL1bip_F3C, CENPAmelL1bip_R2c, and mel_CENPA_PacI R. The *mel* CENP-A^{bipL1} chimera includes residues 1-159 of *mel* CENP-A, 219-232 of *bip* CENP-A, and 175-225 of *mel* CENP-A. Following digestion with AscI and PacI, it was cloned into the pCopia-LAP vector (Cheeseman and Desai, 2005; Erhardt et al., 2008).

The *bip* CENP-A^{melL1} chimera was synthesized as a gBlock (Integrated DNA Technologies), with flanking AscI and PacI sites for subcloning into the pCopia-HA vector.

The *bip-mel* CAL1 chimeras were synthesized as gBlocks with flanking SpeI and NotI sites (New England Biolabs, Inc.) for ligation into the pMT-GFP-LacI vector (Chen et al., 2014; Mendiburo et al., 2011). The *mel* CAL1$^{bip1-160}$ construct includes residues 1-173 of *bip* CAL1 and residues 163-407 of *mel* CAL1. The *mel* CAL1$^{bip1-40}$ construct includes residues 1-40 of *bip* CAL1 and residues 41-407 of *mel* CAL1. The *mel* CAL1$^{bip41-160}$ construct includes residues 1-40 of *mel* CAL1, residues 41-173 of *bip* CAL1, and residues 41-407 of *mel* CAL1. All constructs were verified by sequencing.

Quantification

For experiments in *mel* S2 cells, the localization of GFP or HA-tagged CENP-A or CAL1 orthologs was quantified manually and constructs were classified as either fully centromeric (GFP- or HA-signal co-localized with *mel* CENP-A), diffuse (exclusively euchromatic or cytoplasmic), or centromeric/diffuse (localizing to centromeres and throughout the chromatin). For experiments performed in *mel* lacO S2 cell lines, images were analyzed manually for the presence of the LacI fusion protein on the arms of chromosomes 2 or 3. Only chromosomes showing ectopic GFP (or ectopic CENP-A when using CAL1-LacI without GFP; data not shown) were scored for the presence or absence of centromere/kinetochore proteins. Transient co-transfections in *mel* lacO S2 cells resulted in low n-values (where n equals the number of lacO-positive co-transfected cells) per experiment, due to the polyclonal nature of this cell line combined with transfection efficiency, but 3 biological replicates were performed for each experiment, or 2 when the experiment was repeated with both HA- and GFP-tagged constructs.

Transfection efficiencies in *sim* M-19 cells were significantly lower than in S2 cells, resulting in low n-values (where n equals the number of GFP positive cells) per experiment. 3 biological replicates were performed for each experiment.

For salt extractions, the total centromeric GFP or CENP-C fluorescence signal was found using SoftWorx software (Applied Precision).

Western blots of IPs were quantified using Image Studio Software (Li-Cor) using the Shapes/Quantification function. Intensity of GFP-CENP-A in the IP sample was normalized relative to that of the respective input sample.

Line plots

IF images were quantitatively analyzed in ImageJ using the lines function to create line plots of the endogenous CENP-A and GFP CENP-A fluorescence intensity. Line plots of individual cells were then classified as having diffuse GFP-CENP-A fluorescence (broad signal with no distinct centromeric peak), centromeric/diffuse GFP-CENP-A fluorescence (broad signal with a peak overlapping endogenous *mel* CENP-A peak), or centromeric GFP-CENP-A localization (low background with a distinct centromeric peak).

Multiple sequence alignments

Multiple sequence alignments were performed using the Geneious ® 8.1.5 software (Kearse et al., 2012) using a BLOSUM80 (Eddy, 2004; Henikoff and Henikoff, 1992) cost matrix with free end gaps.

Statistical analyses

All statistical tests were performed using GraphPad ® scientific software. All p-values, with the exception of Figure S4, were calculated using a Fisher's two-tailed test. For Figure S4, p-values were calculated using an unpaired t-test (O'Mahony, 1986).

Supplemental References

Cheeseman, I.M., and Desai, A. (2005). A Combined Approach for the Localization and Tandem Affinity Purification of Protein Complexes from Metazoans. Sci. Signal. *2005*, pl1–pl1.

Chen, C.-C., Dechassa, M.L., Bettini, E., Ledoux, M.B., Belisario, C., Heun, P., Luger, K., and Mellone, B.G. (2014). CAL1 is the Drosophila CENP-A assembly factor. J. Cell Biol. *204*, 313–329.

Chen, C.-C., Bowers, S., Lipinszki, Z., Palladino, J., Trusiak, S., Bettini, E., Rosin, L., Przewloka, M.R., Glover, D.M., O'Neill, R.J., et al. (2015). Establishment of Centromeric Chromatin by the CENP-A Assembly Factor CAL1 Requires FACT-Mediated Transcription. Dev. Cell *34*, 73–84.

Eddy, S.R. (2004). Where did the BLOSUM62 alignment score matrix come from? Nat. Biotechnol. *22*, 1035–1036.

Erhardt, S., Mellone, B.G., Betts, C.M., Zhang, W., Karpen, G.H., and Straight, A.F. (2008). Genome-wide analysis reveals a cell cycle-dependent mechanism controlling centromere propagation. J. Cell Biol. *183*, 805–818.

Henikoff, S., and Henikoff, J.G. (1992). Amino acid substitution matrices from protein blocks. Proc. Natl. Acad. Sci. U. S. A. *89*, 10915–10919.

Kearse, M., Moir, R., Wilson, A., Stones-Havas, S., Cheung, M., Sturrock, S., Buxton, S., Cooper, A., Markowitz, S., Duran, C., et al. (2012). Geneious Basic: an integrated and extendable desktop software platform for the organization and analysis of sequence data. Bioinforma. Oxf. Engl. *28*, 1647–1649.

Mendiburo, M.J., Padeken, J., Fülöp, S., Schepers, A., and Heun, P. (2011). Drosophila CENH3 Is Sufficient for Centromere Formation. Science *334*, 686–690.

O'Mahony, M. (1986). Sensory evaluation of food: statistical methods and procedures (New York: M. Dekker).

Perpelescu, M., Nozaki, N., Obuse, C., Yang, H., and Yoda, K. (2009). Active establishment of centromeric CENP-A chromatin by RSF complex. J. Cell Biol. *185*, 397–407.